The Thesis Committee for Margaret Byers
Certifies that this is the approved version of the following thesis:

Optimization of the Passive Recovery of Uranium from Seawater

APPROVED BY
SUPERVISING COMMITTEE:

Supervisor:

Erich Schneider

Sheldon Landsberger

Optimization of the Passive Recovery of Uranium from Seawater

by

Margaret Elise Byers, B.S.

Thesis

Presented to the Faculty of the Graduate School of

The University of Texas at Austin

in Partial Fulfillment

of the Requirements

for the Degree of

Master of Science in Engineering

The University of Texas at Austin

August 2015

Dedication

This thesis and the supporting work is dedicated to optimism and faith in the evolution of science and technology.

Acknowledgements

I would firstly like to thank my (very soon to be at time of writing) husband for all of his love and support.

Secondly I would like to thank everyone in the Nuclear and Radiation Engineering Program at UT, especially Dr. Schneider for all of his guidance and patience. Additionally, this thesis would not be possible without all of the hard work, intellect, and dedication provided by project collaborators at ORNL and PNNL along with universities partners.

Abstract

Optimization of the Passive Recovery of Uranium from Seawater

Margaret Elise Byers, M.S.E.

The University of Texas at Austin, 2015

Supervisor: Erich Schneider

The aim of this thesis is to optimize the design and deployment conditions utilized by a technology for passively collecting uranium from seawater that is currently under development by Oak Ridge and Pacific Northwest National Labs along with University partners. This system involves the production, deployment, and recycle of an amidoxime ligand grafted onto a high density polyethylene based adsorbent. While many adsorbent performance characteristics and cost inputs impact the final uranium production cost, the system and design parameters explored here include: degree of ligand grafting, number of adsorbent uses prior to ultimate disposal, length of immersion in the sea, and ocean temperature.

Given the complicated empirically-driven nature of the cost calculation, the cost calculation tool is treated as a black box model, thus the minimization requires a derivative free optimization method. A literature review is conducted to explore applicable algorithms and the Nelder-Mead Simplex Method is ultimately selected.

A base case is created using historical values to serve as an initial condition for optimization. From this case, the uranium production cost is minimized, resulting in an

11% decrease. From there, sensitivity cases are considered. An alternative elution process for recovering uranium from the adsorbent is studied. If this innovation can be realized, significant cost savings are shown to be attained if this process fulfills its promise of mitigating adsorbent degradation. Next, the effects of marine bacterial growth on cost are explored. It is determined that optimizing the deployment conditions and improving the uranium binding kinetics can mitigate this increase. Sensitivity analyses are conducted in order to provide insight as to how the optimal deployment conditions are determined.

The results presented in this thesis can inform the direction of future research. Furthermore, as the technology continues to evolve, the methodology developed for this optimization will remain relevant and the optimization too can continue to be used to guide design and R&D decisions.

Table of Contents

List of Tables

List of Figures

INTRODUCTION

The aim of this thesis is to optimize the deployment conditions utilized by a passive uranium collection from seawater that is currently under development by Oak Ridge and Pacific Northwest National Labs along with University partners.

Although much debate surrounds predictions of available future supplies of conventionally mined uranium, it is undeniable that nuclear power as an energy source would benefit from increased supply security. Due to its relatively high solubility in water, uranium is present in the ocean at a concentration of 3.3 ppb [1].

While this low concentration hinders the economic feasibility of its recovery, the magnitude of uranium contained in the oceans, some 4 billion tonnes, would have a transformative effect on issues of supply security. At their current state of maturity, technologies for uranium recovery from seawater chiefly serve to establish a production cost ceiling for uranium. That being said, there is great interest in reducing this cost along with its uncertainty.

This analysis considers an adsorbent that consists of a high density polyethylene (HDPE) backbone co-grafted with an amidoxime ligand to afford uranium affinity and a co-monomer to increase hydrophilicity. The buoyant adsorbent is deployed in the ocean in a kelp field like structure. After a predetermined period of time it is winched up so the uranium may be eluted off the braids. Functional groups on the braids then need to be regenerated with an alkaline solution before they can be re-deployed. This process is repeated until it is no longer economically advantageous to continue to re-use the adsorbent due to the degradation it suffers with each re-use.

The uranium production cost is estimated by considering the costs incurred by one unit mass of adsorbent over its lifetime. This cost has several components, the first of

which is associated with the initial production of the adsorbent. To this is added the cost of mooring a unit mass of adsorbent to the ocean floor, winching it back up, and transporting it to the mothership for elution. Finally, there are costs associated with the removal and purification of the uranium and regeneration of the adsorbent before its next deployment. In all of these process steps the capital, operating, and decommissioning costs are calculated and summed using discounted cash flow techniques similar to those used in previous economic models, specifically Schneider and Sachde [2].

The unit cost of producing uranium is a function of the performance of the technology for adsorbing uranium from the ocean, which is in turn affected by many specific cost drivers. Given all of the feedbacks between adsorbent production options, deployment conditions, and adsorbent performance, the determination of the optimal deployment scenario is non-trivial. As this technology continues to evolve and progress to more detailed stages of the design process, the number of cost driving design parameters will increase. For that reason, manual optimization of system parameters to minimize uranium production cost will become increasingly impractical.

Given the complicated empirically-driven nature of the cost calculation, the cost calculation tool will be treated as a black box model, thus the minimization requires a derivative free optimization method. A literature review is conducted to explore applicable existing algorithms. Then case studies of other engineering cost minimizations are considered and compared to the optimization problem at hand. Finally an algorithm is selected and used to find the optimal conditions for a predefined base case along with additional permutations of the base case. Verification of the method is achieved by comparing the solutions to a brute force calculation using discrete values for the decision. Finally sensitivities to various input parameters and process costs are explored.

The cost calculation and optimization tool is developed with a graphical user interface to make the calculation more transparent to the technologists and system designers who will be its main users. Interacting with the cost calculation and seeing the biggest cost drivers permits users to further optimize the chemistry to subsequently lower the uranium recovery cost. Coupling of the cost analysis tool with an optimization algorithm will therefore guide future research and development decision-making, as the tool will point the way toward design choices that would have the most substantial cost benefits.

LITERATURE REVIEW

Optimization Methods

SIMULATED ANNEALING

Simulated annealing turns to statistical mechanics to solve combinatorial optimization problems. The process of metal atoms continually rearranging in order to find the lowest energy configuration as the temperature of the system is slowly lowered is simulated. A cost function, in this case the cost of uranium from seawater, is analogous to the energy of the system as both are to be minimized in the optimal solution. The random movement of atoms is modeled through the iterative process of randomly selected parameter values, moving forward with those which lower the cost function. In order to escape local minima, configurations that increase the cost function relative to the previous iteration are accepted with a probability dictated by the Boltzmann distribution as seen by Equation 2.1.

$$P(\Delta E) = e^{\frac{\Delta E}{k_B T}} \tag{2.1}$$

In the case of simulated annealing, the temperature is slowly lowered, allowing the system to reach steady state at each temperature decrement until the system "freezes" and the reconfigurations cease [3].

Simulated annealing has the benefit of the statistical guarantee of finding the optimal solution, even for cost functions that are nonlinear of discontinuous. It is also praised for its ability to handle boundary conditions. Its biggest drawback is often cited as being very time consuming. It is also criticized as being difficult to fine tune to specific problem [4].

GENETIC ALGORITHM

The genetic algorithm is based off the theory of evolution where iterative generations work toward an optimal solution. It begins with an initial random population of "chromosomes" all of which are given a fitness value. The fitness value is a ratio of a given solutions objective value function, f_i, to the average evaluation of the current population: $f_i/\bar{f}$. This ratio is used to create the intermediate population where any chromosome whose fitness is greater than one is copied to the intermediate generation; the value by which the fitness is greater than 1 is the probability that a second copy is placed in the intermediate population. Chromosomes with fitness less than one are accepted to the intermediate generation with probability equal to their fractional fitness value. To create the next generation, mutation and cross over are simulated by randomly pairing solutions referred to as the parent chromosomes. There is a probability that these two solutions will be recombined to form an offspring, all of which are subject to mutation by a very low probability, often set to less than 1%.

A drawback of the genetic algorithm is that it does have the potential to get stuck in local optima, although the mutations are introduced as an attempt to counter-act this [5]. Also, all genes or parameters must be converted into binary numbers so that chromosomes can be recombined in the form of binary strings. This extra step can become quite a computational challenge.

ANT COLONY OPTIMIZATION

Ant colony optimization methods mirror the collective nature of individual ants unknowingly working together to increase survivability of the colony. As ants travel away from their nest in search for food they leave chemical pheromones telling other ants where they have traveled. As shorter, more optimal paths are found, ants will continually travel these paths, subsequently increasing the pheromone concentration, thereby

prompting more ants to converge to this optimal path. This positive feedback is further supported by the fact that pheromones evaporate over time, thus leading to lower pheromone densities on longer paths as longer travel times leads to more evaporation. This process is simulated by iteratively distributing pheromone, τ_i, to possible solutions according to Equation 2.2.

$$\tau_i = \tau_i + \frac{Q}{f(s)} \tag{2.2}$$

Solutions having a lower value of the objective function, f, get a higher pheromone density, representative of a fixed number of pheromones, Q, being distributed over varying path lengths [6].

The main benefit of the ant colony optimization method is that it strikes a balance between random and directed search due to the feedbacks systems. The evaporation of pheromones on long, infrequently traveled paths provides a negative feedback while an optimal solution will increase in pheromone density, eventually converging on the solution. It is possible to converge on a less optimal solution. Also, this method is criticized of inefficiently using previously acquired information, taking longer to reach a solution [7].

NEWTON'S METHOD

Newton's method is an iterative root finding approach commonly used for solving nonlinear optimization problems due to its simplicity and robustness, given a good initial guess. Newton's method is based off of a Taylor approximation at a given point of the objective function, f, giving an approximation of the tangent line as displayed in Equation 2.3.

$$f(x_{i+1}) \approx f(x_i) + f'(x_i) * (x_{i+1} - x_i) \tag{2.3}$$

This is then rearranged (Equation 2.4) by setting the x-intercept as the next point to give the formula for step size

$$x_{i+1} = x_i - \frac{f(x_i)}{f'(x_i)} \tag{2.4}$$

which can easily be generalized to multiple dimensions by replacing$f'(x_i)$ with the Jacobian matrix, of partial derivatives of the cost function and replacing x with a vector containing the ith parameters values.

Often times, as in the case of uranium from seawater, it is not the root of the recovery cost function but instead the minimum that is desired. Therefore the method is actually applied to the derivative of the function$f(x_i)$ to find the zero of $f'(x_i)$, i.e. the minimum of the original function. The second order approximation of this Taylor series is seen in Equation 2.5.

$$f'(x_{i+1}) \approx f'(x_i) + f''(x_i) * (x_{i+1} - x_i) \tag{2.5}$$

This can likewise be manipulated to find the zero of the derivative using the update model shown in Equation 2.6

$$x_{i+1} = x_i - \frac{f'(x_i)}{f''(x_i)} \; or \; x_{i+1} = x_i - \frac{J_i}{H_i} \tag{2.6}$$

This appears problematic in that the analytical derivative of the cost function is unobtainable, but can be approximated via finite differencing. This is done by estimating the Jacobian,J, and Hessian, H, of the cost function using finite differencing. Central

differencing using a predetermined step size, h, is implemented according to Equations 2.7-2.9.

$$J_i = \frac{f(x_i + h_i) - f(x_i - h_i)}{(2h_i)} \tag{2.7}$$

$$H = \begin{bmatrix} \frac{d^2f}{\delta d^2} & \frac{d^2f}{\delta d \delta n} \\ \frac{d^2f}{\delta n \delta d} & \frac{d^2f}{\delta n^2} \end{bmatrix} \tag{2.8}$$

$$\frac{d^2f}{dx_i dx_j} = \frac{f\left(x + h_i e_i + h_j e_j\right) - f\left(x + h_i e_i - h_j e_j\right)}{4h_i h_j} - \frac{-f\left(x - h_i e_i + h_j e_j\right) + f(x - h_i e_i - h_j e_j)}{4h_i h_j} \tag{2.9}$$

Although this approximation does introduce additional error, as long as the step size is small then this finite difference approximation will be reasonably close to the true Newton's method. This does however require additional calculations of the cost function, which can slow down the process [8].

The benefit of Newton's method is its simplicity and its quick convergence when in the vicinity of the optimal solution. However, a poor initial guess can lead to a slow or even failed convergence, especially if the gradient is near 0. This is potentially a problem with respect to the optimization of uranium production cost as the cost seems to plateau with high number of uses and length of campaign. In an attempt to fix this problem a step size, σ, is often added. For efficiency, sigma can be calculated via the quadratic approximation in Equation 2.10

$$\sigma = \frac{J^T * s}{s^T * H * s} \tag{2.10}$$

where s is the step direction calculated with the Newton step.

NELDER-MEAD SIMPLEX METHOD

This method follows the directed movement of a simplex, a shape of n+1 vertices in n dimensions, through the parameter space until it arrives at the minimum. The number of dimensions corresponds to the number of decision variables being optimized. Each vertex, P, represents a set of decision variables and their associated objective function value. With each iteration the simplex moves through the feasible region by replacing at least one vertex with a new set of conditions and their objective function value. The following description is based off the original published by the creators of the method, which assumes that the objective function is to be minimized [9].

An iteration begins by ordering the vertices with respect to increasing objective function values. The point corresponding to the lowest valued objective function is denoted as P_l and the that with the highest value as P_h. The centroid, $\bar{P}$, of the points of the n-1most desirable objective function values , i.e. vertices P_i $i \neq h$, is calculated to be used in the transformation. A new vertex is found by reflecting the simplex at point P_h across the centroid and is hence referred to as the reflection point, P_r and is calculated as seen below. This reflection is depicted both mathematically in Equation 2.11 and illustratively in two dimensions in subsequent figures below, beginning with Figure 2.1.

$$P_r = \bar{P} + \alpha(\bar{P} - P_h) \tag{2.11}$$

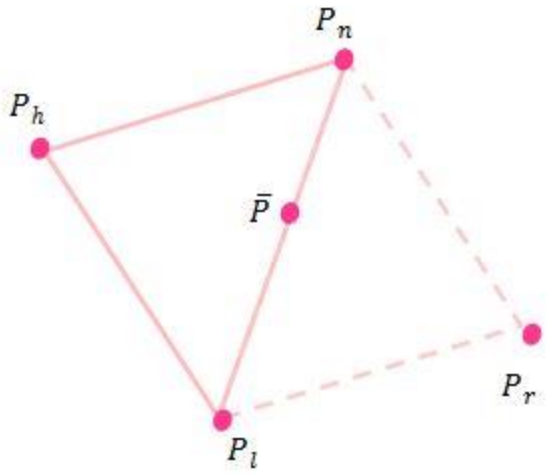

Figure 2.1: Reflection of the Simplex

The parameter values corresponding to this reflection point are used to calculate the corresponding objective function value so that the way in which the simplex moves can be determined.

If the reflection cost lies between the lowest and second highest P_n, vertices then the least favorable vertex, P_h, is replaced with the reflection point and the iteration repeats.

If the reflection cost is better than the best vertex, P_l then the simplex is temporarily extended to see if the algorithm is moving in a very favorable direction. The extension point, P_e, is calculated in the same way as the reflection point except that change in each parameter is multiplied by an expansion coefficient, γ,. The formula for determining the extension point is shown in Equation 2.12 and the two dimensional representation in Figure 2.2.

$$P_e = \bar{P} + \alpha\gamma(\bar{P} - P_h) \tag{2.12}$$

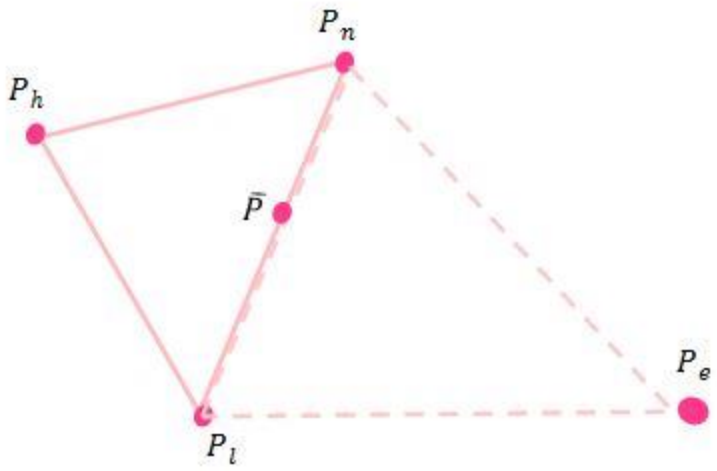

Figure 2.2: Expansion of the Simplex

If the cost yielded by the extension point is even smaller than the reflection point then the extension point replaces the point P_h and the iteration is over. Otherwise, if the expansion is not favorable, the point P_h is replaced with the reflection point and the algorithm repeats.

If the reflection cost is between the highest and second highest vertices then the simplex is temporarily contracted. The contraction point, P_c, is calculated in the same way as the extension point but is instead controlled by the contraction coefficient, β (Equation 2.13 and Figure 2.3).

$$P_c = \bar{P} + \alpha\beta(\bar{P} - P_h) \tag{2.13}$$

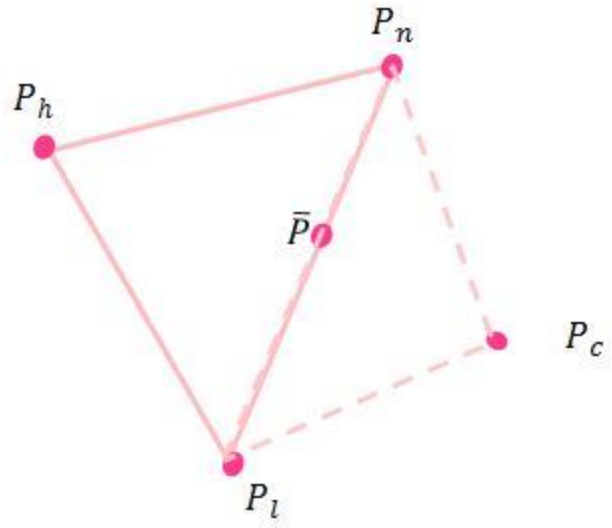

Figure 2.3: Outward Contraction of the Simplex

The contraction coefficient must be less than one in order to decrease the volume of the simplex. If the contraction point yields a cost that is less than that of the reflection point, then P_c replaces the worst vertex P_h. However, if the bojective function value at the contraction point is greater than its value at the reflection point then the simplex is shrunk, the process for which will be described below.

If the reflection cost is greater than that of the highest vertex then the simplex is again temporarily contracted, but this time in the opposite direction. This inner contraction is toward the point P_h as opposed to toward P_r. This other contraction point, P_{cc}, is calculated in much the same way as the first contraction point but without the reflection coefficient (Equation 2.14 and Figure 2.4).

$$P_{cc} = \bar{P} - \beta(\bar{P} - P_h) \tag{2.14}$$

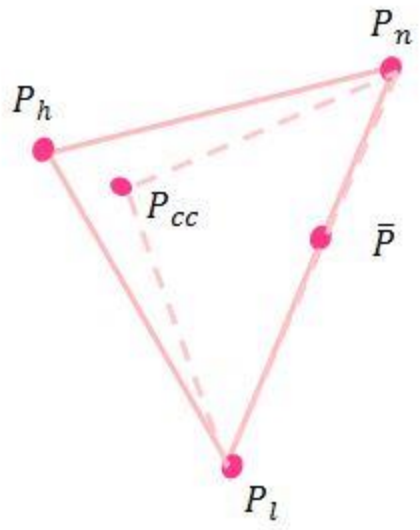

Figure 2.4: Inward Contraction of the Simplex

If the objective function at this new inner contracted point P_{cc} is more favorable than the least favorable vertex, P_h, then P_{cc} replaces P_h and the iteration terminates. Otherwise the simplex is shrunk.

The simplex shrinks in size when a contraction fails by providing a higher cost than the existing vertices. To avoid moving away from a minimum, n new vertices are computed to bring the simplex closer to the smallest objective function value,P_l, discovered so far. These new points, P_i, are computed as shown by Equation 2.15 and Figure 2.5.

$$P_i = P_l + \delta(P_i - P_l) \tag{2.15}$$

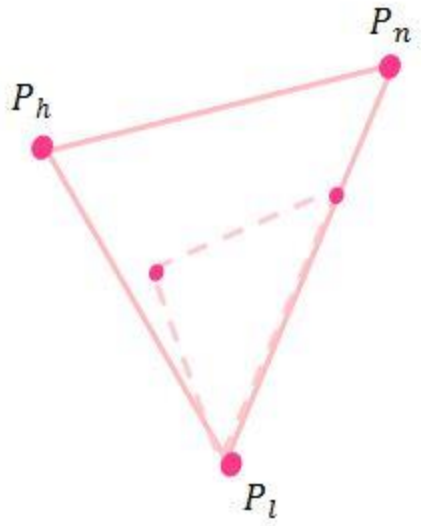

Figure 2.5: Shrinking of the Simplex

where $i = 2{:}\, n + 1$

The convergence criteria used to terminate the method is based on the objective function values since no derivatives are available for the determination of a stationary point. The process ends when the objective function values at all vertices are approaching the same value. This is achieved when the standard error of the objective function values, ε, at the given simplex fall below a predetermine epsilon value. At each iteration this convergence criteria is check using Equation 2.16

$$\varepsilon = \sqrt{\sum \frac{(y_i - \bar{y})^2}{n}} \tag{2.16}$$

Case Studies

Leps and Sejnoha [10] use a combination of a genetic algorithm and augmented simulated annealing to optimize the design of steel reinforced concrete structures. The authors combine the principles of these two techniques by optimizing on a population as opposed to a single point while guiding the search toward minimal energy states. This starts with transforming all parameters into binary strings, as is required for use in a genetic algorithm. Parent chromosomes are selected for reproduction according to their fitness function. Fit parents then recombine via uniform crossover with mutation applied randomly to the offspring with small probability. In order to avoid becoming trapped in a local minimum, the offspring are then accepted according to a probability dependent upon their fitness function and a temperature. If the fitness of the new individual is greater than that of the previous than the new solution always replaces the old one. As the temperature decreases with time, the probability of a less fit solution replacing its more fit parent increases.

Jayabalan and Chadhuri [11] attempt to minimize maintenance cost for systems required to achieve, or fall below, acceptable failure rates. Failures are avoided by 2 different types of preventive maintenance at predetermined points in time, subject to inflationary trends over the considered time horizon. The 2 types of maintenance include a simple servicing and preventive replacement, with the latter being the more expensive and thus least desirable of the two. Therefore, in order to minimize the scheduled cost, a solution containing the optimal number of simple maintenances performed before a replacement is found using a branching algorithm.

The branching algorithm begins by branching the search space into smaller sets of possible solutions. These nodes are then bound by determining the upper

and lower bound of the minimum value of the objective function. The nodes are then iteratively "pruned" by rejecting those nodes whose lower bound is greater than the upper bound of a reference node. In the case of the maintenance cost as the objective function, the nodes are pruned by comparing not only the total maintenance cost, but also the time between replacements, which must be greater than that of the reference solution. This process is repeated as the number of nodes decreases until convergence on the optimal solution is achieved.

Sanatarelli and Pellegrino [12] use a downhill simplex method in order to optimize a renewable energy plant. In this case the objective function is the investment cost of the plant, which is required to meet a set electricity demand. Although the analytical form of the cost function is known, a black box optimization approach is used since the constraints are not analytically tied to the decision variables but are instead logical based through a nested simulation.

The authors' literature review directed them toward the commonly used class of Evolutionary Algorithms, notably the Powell and Simplex methods. Although neither algorithm requires use of a derivative and the Simplex is not necessarily the quickest to converge, the Simplex method was chosen for its reputation of efficiency and robustness. The Downhill Simplex Method essentially moves a simplex through the parameter space, eventually finding a minimum. An initial simplex, a geometrical shape of N dimensions containing N+1 vertices, is chosen as the starting point. Progression from this starting point is made by one of three types of steps through the topography: reflection, contraction moves, or expansion moves. The simplest of these is reflection moves, in which the highest point of the simplex, where the objective function is largest, is reflected through the opposite face to what is presumably a lower point, P_r. If this new point, P_r, is bracketed between the simplex vertices having the second highest and lowest objective

function values, then this becomes the new simplex, which has the same volume as the one in the previous step. If however, the point P_r yields an objective value function lower than or equal to that of the lowest point in the simplex, then the value of the objective function is determined at a point P_{rr}. This new point is even further away from the initial point in the direction of P_r, expanding the simplex. The lowest value amongst P_r and P_{rr} then replaces the highest point of the initial simplex. Contrastingly, if the reflection point values the objective function greater than or equal to that of the highest simplex point, then simplex is contracted toward the centroid of the N-1 dimensional shape made up of all simplex points, except the highest one to new point, P_{rr}' If the function at point P_r is between that of the highest and second highest simplex points, then the function is valued at a point P_{rr}'', essentially a reflection of point P_{rr}' across the opposite face. If the objective function is lower at P_{rr}' or P_{rr}'' than the highest simplex point, then it replaces the highest point. However if the value is higher than that of the highest point or the reflection point, then the simplex contracts in all directions, honing in on its minimum.

Abendroth and Salmon [13] optimize the cost of designing restrained end reinforced concrete T-sections. Similar to the cost of uranium from seawater, the total cost of these beams is a function of multiple design parameters, each with their own constraints. In this analysis the objective function was minimized by first transforming the problem to an unconstrained minimization. This was done using an internal penalty function, or an additional term in the original cost function that provides the new objective function of the unconstrained problem. The penalty function is a quantitative measure of the violation of the constraint, such that the value is zero when the parameters are within the constraints.

The unconstrained optimization problem was then solved using a quasi-Newton method. The Fletcher-Power method was employed by approximating the inverse of the Hessian. This method requires the use of the first partial derivative of the cost function, which in the case of these T-sections was believed to be easier to solve in closed form than via finite differencing. The change in the gradient is then used to update the estimate for the inverse Hessian.

Reflection of Case Studies

In order to down select from the various optimization techniques available, the merit of each approach as it applies to the optimization of the cost of uranium from seawater is considered. This comparison is organized qualitatively in Table 3.1.

Table 3.1: Comparison of Potential Optimization Methods

Algorithm	Complexity	Ability to Converge on Global Minimum	Ease of Coupling to Black Box Model
Simulated Annealing	Medium	High	Low
Genetic	High	Medium	Low
Ant Colony	High	High	Medium
Newton	Low	Medium	Medium
Nelder-Mead Simplex	Medium	High	High

The first case examined, Lips and Sejnoha's [10] optimization of concrete structure design to minimize cost, does not appear to be the best method for the minimization of uranium cost. The genetic algorithm is notorious for difficulty of coding, and therefore given the time and resource constraints of this project, is likely not the best fit. If significant weight is to be given to this consideration, the perhaps the best path to follow would be that of Abendroth and Salmon [13] with their use of a quasi-Newton method. Unlike their attempt however, the Jacobian, along with the Hessian,

will be approximated using finite differencing as finding these in closed form is essentially not feasible.

METHODOLOGY

In the case of uranium from seawater, the objective function is made up of a combination of multiple both scalar and non-scalar functions. The tool used to compute the uranium production cost is an excel spreadsheet with many built-in dependencies and conditional operations. The complexity and form of this calculation make it such that only black box optimization is possible.

This methodology will first describe the black box used to calculate the uranium production cost, although it is not directly relevant to the optimization. Secondly, the optimization will be discussed. The explanation will begin by describing the parameter space, and then the actual optimization algorithm will be described in greater detail.

Cost Estimation Methodology

This economic analysis provides an estimate of the cost to recover uranium from seawater on an industrial scale via a passive collection process currently under development at Oak Ridge and Pacific Northwest National Labs (ORNL and PNNL). The proposed system consists of three major steps whose costs were considered individually and then summed. First the fibrous adsorbent must be produced via radical polymerization. Once braided, the adsorbent is then sent out to sea to be moored to the bottom of the ocean. After a pre-determine collection period the loaded adsorbent is retrieved and the uranium is eluted off in a chemical bath and the process repeated until it is no longer economically advantageous to continue.

The capital, operating, and decommissioning costs associated with the three major steps are evaluated, and a timeline of when the costs are incurred is developed. These are then summed using a discounted cash flow technique, wherein the time value of money is taken into account [14]. Other common engineering economics

methods were included such as economies of scale and the use of Monte Carlo propagation of error.

The following methodology will depict the procedure used to calculate the net present value of the costs associated with the recovery of uranium from seawater, relying primarily on the EMWG cost estimation guidelines as a reference (EMWG 2007). This cost estimate will depend on a discounted cash flow technique to track the lifecycle of a unit mass of adsorbent from its initial fabrication through its re-uses and final disposal. This explanation will begin with a wide scope by describing the general methodology used to calculate the unit cost of uranium, given all of the process costs. Then, the details regarding the calculations of the individual cost inputs for each step in the lifecycle of the reference adsorbent will be discussed in higher fidelity.

DISCOUNTED CASH FLOW

A lifecycle discounted cash flow approach adjusts costs according to the time value of money via the discount rate, r, which for this analysis will be set at 7%. Capital expenses will be made payable on a schedule derived using the amortization factor, *AF*, which is a factor of the interest rate on capital, i_c, and the length of time over which the debt is financed, t_{proj}, as seen in Equation 3.**Error! Reference source not found.**.

$$AF = \frac{\left(1 - \frac{1}{1 + i_c}\right)^{t_{proj}}}{i_c} \tag{3.1}$$

This technique also requires that a point in time be set as time zero, so that all prior and subsequent costs may be discounted to that reference time in accordance with the time value of money [14]. This lifecycle discounted cash flow analysis sets time zero

to be the point of initial deployment of a unit of adsorbent. All costs are assumed to be incurred when they are encountered in the lifecycle, e.g., all components of the nth elution are paid when a unit mass of adsorbent is eluted for the nth time. This analysis considers steady state operations, so all unit masses of adsorbent are treated as having a timeline identical to the one shown in Figure 3.1.

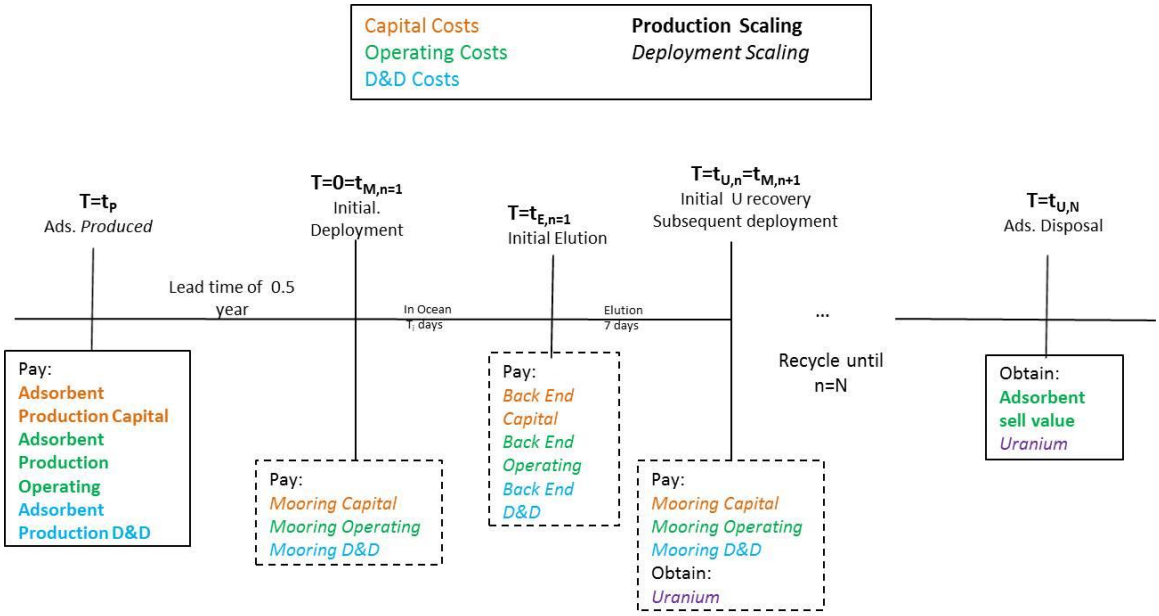

Figure 3.1: Adsorbent Lifecycle Timeline

Each cost component is calculated for the various process steps and then normalized to common units, which may be cost per ton of adsorbent produced or cost per ton of adsorbent deployed depending on the process step. All cost components for a given system process are then summed together to give a unit cost for each process, also having units of cost per ton of adsorbent produced or deployed. In the case of mooring and back end costs, unit costs are then discounted from the future time at which each use occurs back to the present, and summed over all N uses to yield the lifecycle unit cost of

these processes. Adsorbent production and disposal however only occur once in the lifecycle so their unit costs are simply discounted to the past or future, respectively. All system steps are summed to give the total lifecycle cost for a unit of adsorbent. The total lifecycle cost of adsorbent, luc_{ads}, is then simply divided by the discounted uranium recovery rate per unit adsorbent, l_c, to yield a final cost of uranium as in Equation 3.2

$$uc_u = \frac{luc_{ads}}{lc} \tag{3.2}$$

The remainder of this section describes in detail the procedures for calculating luc_{ads} and $l_c$using the values derived in the subsequent cost input section for overnight capital and annual operating cost of each task in the lifecycle.

Adsorbent Production

Capital Costs

The first cost element calculated is a unit mass of adsorbent's share of the total amortized capital cost for the adsorbent production facility. The capital cost includes all cost encountered prior to the initiation of facility operations. In this case of adsorbent production, the main components of this cost include the buildings and equipment used for manufacturing the adsorbent backbone, grafting the ligand, and braiding and conditioning before going out to sea. The details regarding the data and calculation of this overnight cost can be found in the cost input section of the methodology and the data section in Appendix A.

The annual throughput of the facility, m_{prod}, is an important parameter not only in dictating the size or number of units of equipment, but also in finding the distribution of capital cost among all units of adsorbent. The demand for adsorbent production is a

factor of the annual uranium requirement, U_{req}, along with the total lifetime capacity of the adsorbent, C_{tot}, as calculated in Equation 3.3.

$$m_{prod} = \frac{U_{req}}{C_{tot}} * \frac{1000kg}{ton} \tag{3.3}$$

The overnight capital cost,OCC_{prod}, having units of dollars, is financed by amortization over the project lifecycle. This amortization process is a function of the interest rate and project lifetime, or more compactly the amortization factor derived earlier (Equation 3.1), and is done according to Equation 3.4, yielding an annual cost, CC_{prod}, for adsorbent production.

$$CC_{prod} = \frac{OCC_{prod}}{AF} \tag{3.4}$$

The annual cost can simply be normalized per unit of adsorbent produced per year to give the capital cost associated with producing one unit of adsorbent, cc_{prod} as shown in Equation 3.5.

$$cc_{prod} = \frac{CCprod}{m_{prod}} \tag{3.5}$$

Operating Costs

Operations and maintenance costs are tabulated on a per unit of adsorbent produced basis by assuming the annual operating costs are already know, as they will be calculated in the subsequent section. This annual cost,OC_{prod}, is a function of materials, labor, utilities, etc., and can be treated similarly to the amortized capital costs, as evident by their corresponding units.

The adsorbent production operating cost for each unit of adsorbent produced, calculated in Equation 3.6, is the quotient of annual operating costs of the adsorbent production facility and the total mass of adsorbent produced each year.

$$oc_{prod} = \frac{OC_{prod}}{m_{prod}} \tag{3.6}$$

Disposal and Decommissioning (D&D) Costs

Finally, upon cessation of the project all of the facilities and equipment must be decommissioned and/or disposed of. This lump sum D&D cost, ODC_{prod}, is estimated to be 10% of the capital cost corresponding to that process step. Similar to the process of annualizing capital payments, the D&D costs are made payable on a yearly basis. Unlike the capital costs that incur a financing fee, the funds set aside for D&D of facilities earn interest in a sinking fund at an annual rate of i_{SF} throughout the project lifecycle. Thus, the annual cost of D&D, DC_{prod}, is a function of the interest rate paid on this sinking fund and can be calculated via Equation 3.7.

$$DC_{prod} = \frac{ODC_{prod} * i_{SF}}{(i_{SF} + 1)^{t_{prod}} - 1} \tag{3.7}$$

Moving forward, the normalized cost, dc_{prod}, can be obtained as outlined above; the annual cost is simply divided by the annual adsorbent production rate as shown in Equation 3.8.

$$dc_{prod} = \frac{DC_{prod}}{m_{prod}} \tag{3.8}$$

Mooring and Deployment

Capital Costs

The capital cost associated with mooring accounts for the expenses applicable to the process of mooring and deploying the adsorbent. Since this part of the process occurs at sea, there is no building cost. Instead the capital cost is derived from the boats and mooring chains needed for operations. These and other input costs are summed in the next section to give the overnight capital cost, OCC_{moor}, used here. The overnight cost is amortized in Equation 3.9 to give an annual expense for the mooring capital, CC_{moor}.

$$CC_{moor} = \frac{OCC_{moor}}{AF} \tag{3.9}$$

Mooring of the adsorbent utilizes a different normalization factor than adsorbent production since each unit mass of adsorbent undergoes the mooring and elution processes N times. Therefore the rate at which adsorbent is deployed in the ocean, m_{dep}, is a factor of N greater than the rate at which adsorbent is produced (Equation 3.10).

$$m_{dep} = U_{req} * \frac{N}{C_{tot}} * \frac{1000kg}{ton} \tag{3.10}$$

The mooring and deployment system capital cost per unit mass of adsorbent deployed in the ocean, cc_{moor}, is then calculated in Equation 3.11 by dividing the annual mooring cost by the total mass of adsorbent deployed per year.

$$cc_{moor} = \frac{CC_{moor}}{m_{dep}} \tag{3.11}$$

Operating Costs

The normalized cost of mooring operations and maintenance are calculated from the annual operating costs derived in the cost input section. The annual operating cost of mooring,OC_{moor}, is divided by the total mass of adsorbent deployed per year in Equation 3.12 to again give cost per unit of adsorbent deployed, oc_{moor}.

$$oc_{moor} = \frac{OC_{moor}}{m_{dep}} \tag{3.12}$$

Disposal and Decommissioning Costs

The D&D cost for mooring and deployment is modeled in largely the same way as the D&D cost for adsorbent production as calculated in Equation 3.13. The overnight D&D cost,ODC_{moor}, is estimated to be 10% of the overnight capital cost and then annualized using the interest rate on the sinking fund to yield the annual expense, DC_{moor}.

$$DC_{moor} = \frac{ODC_{moor} * i_{SF}}{(i_{SF} + 1)^{t_{prod}} - 1} \tag{3.13}$$

The divergence from the adsorbent production method, seen in Equation 3.14, comes when the annual D&D cost is divided by the annual deployment rate, as is the case with the other mooring expenses, arriving at the D&D cost normalized per unit of adsorbent deployed, dc_{moor}.

$$dc_{moor} = \frac{DC_{moor}}{m_{dep}} \tag{3.14}$$

Elution and Regeneration

Capital Costs

The back end capital cost is comprised of the buildings and equipment needed to elute the uranium off of the braided adsorbent and then transform it to ammonium diruanate, along with the re-conditioning necessary to prepare the adsorbent for another deployment. To find the normalized capital cost for this process, the overnight capital cost, OCC_{elut}, derived from the individual inputs is amortized over the production lifetime to yield an annual cost, CC_{elut} as shown in Equation 3.15

$$CC_{elut} = \frac{OCC_{elut}}{AF} \tag{3.15}$$

Since the unit mass of adsorbent is deployed N times, it goes through the back end process N times as well. Therefore the annual expense is normalized per unit of adsorbent deployed to give cc_{elut} (Equation 3.16).

$$cc_{elut} = \frac{CC_{elut}}{m_{dep}} \tag{3.16}$$

Operating Costs

Back end operating costs are a factor of the chemicals, labor, and utilities required, as will be detailed later to find the annual operating cost of elution and reconditioning. The annual operating costs of elution, OC_{elut}, must be divided by the total mass of adsorbent deployed per year to give oc_{elut}, the normalized operating cost. This calculation is shown in Equation 3.17.

$$oc_{elut} = \frac{OC_{elut}}{m_{dep}} \tag{3.17}$$

Worth noting, is that the operating costs for reconditioning are not included in the last use of the adsorbent.

Disposal and Decommissioning Costs

The D&D cost for the back end it analogous to that of mooring and deployment in that it can be found on a per unit of adsorbent deployed basis, which is done in Equation 3.18. The overnight cost, ODC_{elut}, is a fraction of the overnight capital cost, which is then annualized over the project lifetime to give an annual cost, DC_{elut}.

$$DC_{elut} = \frac{ODC_{elut} * i_{SF}}{(i_{SF} + 1)^{t_{prod}} - 1} \tag{3.18}$$

The annual D&D cost is normalized in Equation 3.19 to units of adsorbent deployed.

$$dc_{elut} = \frac{DC_{elut}}{m_{dep}} \tag{3.19}$$

Unit Cost

Cost Input Calculations

In the previous section it was assumed that the overnight capital cost and annual operating cost of each of the process tasks was known in order to carry out the discounted cash flow analysis. This section will detail how those costs were derived and the value of said costs will be tabulated in Table A1. Much of the data and methodology was taken from a previous thesis [15] describing the cost calculation and updated to reflect the current process. This section will only address the changes made so if a cost is not mentioned here then it can be assumed to be calculated in the same way as [15].

In all cases, the overnight capital costs are a sum of all costs incurred prior to the commencement of operations, including buildings, equipment, one month's worth of initial inventory, along with other miscellaneous costs. Storage tanks are sized for one month's worth of chemical usage; the cost to stock these tanks is folded into the capital so that the facility can begin production as soon as construction commences. The annual operating costs are a function of the labor, materials, utilities, and maintenance costs of each process.

Both top-down and bottom-up estimations will be used, depending on the level of available details for each cost element. Bottom-up modeling is more suitable for a well-developed technology; it is often employed when a project approaches construction and thus has a detailed and relatively accurate list of inputs and their costs. Conversely, a top-down estimate is used for projects in early developmental stages, with a large degree of uncertainty. Since the required commodities, equipment, and their costs are not known to a great level of detail, similar projects, consisting of parallel equipment and steps, provides estimates of these analogous steps. These estimates of a similar piece of equipment, for example, are then appropriately scaled to obtain the cost to provide the

desired through put [16]. The scaling factors vary among equipment type, with the standard .67 being used when not enough information is available to generate technology specific factors. The scaling factors used in this analysis can be found in Table A2 of the Appendix.

Adsorbent Production

Overnight Capital Cost

In the case of the adsorbent production facility the aspects of the capital cost were derived from existing and theoretical chemical plants that were scaled in order to produce the desired annual adsorbent output, m_{prod}, determined previously. Since the adsorbent consists of two components, backbone fiber and ligand, some inputs scale specifically to the throughput of just one of these parts, as determined by the degree of grafting, *g,* calculated in Equation 3.**Error! Reference source not found.**0, or the entire mass of inished adsorbent.

$$g(\%) = \frac{W_f - W_i}{W_i} * 100\% \tag{3.20}$$

The melt spinning and e-beam irradiation equipment used to produce the fibers scales with the amount of HDPE fiber required to produce the desired finished adsorbent output. Similarly, the resources used for the grafting of the amidoxime scale with the amount of ligand required to produce the desired finished adsorbent output. Other miscellaneous factors such as land, contractor's fees, and electrical systems are estimated to be a fraction of the equipment cost, and thus scale with the throughput of finished adsorbent. All of the data for the aforementioned factors were determined as outlined in Table A3 of Appendix A and then summed up to obtain the overnight capital cost, OCC_{prod}.

Annual Operating Cost

Similar to capital costs, components of the operating cost, notably chemicals, scale according to the annual throughput of HDPE and/or ligand, depending on their role in the manufacturing process. Unlike in the case of the capital costs, chemicals scale directly proportional to HDPE or ligand production, rather than via a scaling factor. All chemicals are assumed to be used with 100% efficiency of their nominal, often stoichiometrically derived, values, which are tabulated in Appendix A (Table A4). Some chemicals are known to be reusable. The degree to which they are recycled is 90% to account for some inevitable loss. Both of these values are assumptions that may not necessarily provide a conservative estimate of reality. Costs categorized as miscellaneous, such as taxes, contingency, etc., scale with the production rate of finished adsorbent. The cost of hazardous waste disposal is included using incineration as the disposal method for select chemicals. The data used for these costs can be found in Appendix A.

Mooring and Deployment

Overnight Capital Cost

The overnight capital cost associated with mooring and deployment of adsorbent is a sum of the cost of all of the required boats and mooring chains. The deployment strategy currently incorporated into the cost model is that of the off-shore elution described in [17]. The number of work boats and chains required to obtain the annual uranium requirement is a function of the adsorbent uptake. As mentioned in the reference, there is only one mother ship and one supply ship. The size of these two ships is scaled by the uranium recovery, and thus adsorbent uptake. Specific data and calculations for these parameters can be found in Appendix A and reference [17].

Annual Operating Cost

The operating cost for mooring and deployment is driven primarily by the fuel consumption of the boats. The other components in this sum are the labor required to operate the ships, and the off-shore lease, all of which depend indirectly upon adsorbent uptake. The area required for the adsorbent field is also a function of adsorbent spacing. These relationships and reference data can be found in Table A10 and references [15] and [17].

Elution and Regeneration

Overnight Capital Cost

The overnight capital cost for the elution and reconditioning step is a sum of the expenses encountered in building the facility, stocking it with the necessary equipment and initial inventory, along with the miscellaneous costs. The elution equipment scales with the mass of adsorbent that must be eluted each year. The digestion and solvent extraction equipment however scale with the mass of uranium required each year, and are thus unique from many other cost components in that they are independent of adsorbent uptake. Similar to the adsorbent production capital cost, one month's worth of initial chemical inventory is included in the capital cost. Miscellaneous costs, similar to those in adsorbent production, are also included and scale with the total equipment cost. Details regarding these calculations can be found in the Appendix and [15].

Annual Operating Cost

The operating cost components, as in the capital cost, scale with their respective roles in the back end processing. It is worth pointing out again that the reconditioning of the adsorbent only happens when the adsorbent is to go back into the ocean, and thus takes place N-1 times. These chemicals are again assumed to be used with 100%

efficiency and 90% recyclability. Scaling for the components summed in the annual operating cost were derived from reference thesis with specifications detailed in Appendix A.

Parameter Space

Length of Campaign

The relationship governing adsorbent uptake as a function of immersion time is described as follows. The uranium complexation with amidoxime is presumed to follow the one site ligand saturation model shown in Equation 3.21 according to [18]. The maximum uptake of the adsorbent before accounting for secondary effects like degree of grafting and degradation, C_{max}, is dictated by two measured characteristics of the adsorbent: the theoretical saturation capacity, β_{max} , and the half saturation time, K_D. As a function of the length of campaign, t_i the one-site ligand saturation model is given by

$$C_{max} = \frac{B_{max} * t_i}{K_D + t_i} \tag{3.21}$$

The values for saturation capacity and half saturation time are unique to the adsorbent and must be determined experimentally. Time series data for uranium uptake received from ORNL is fitted to the one site ligand saturation model to yield values for K_D and β_{max} of 25.9 days and 4.6 g U/kg ads respectively, giving rise to a relationship between length of campaign and adsorbent as depicted in Figure 3.2.

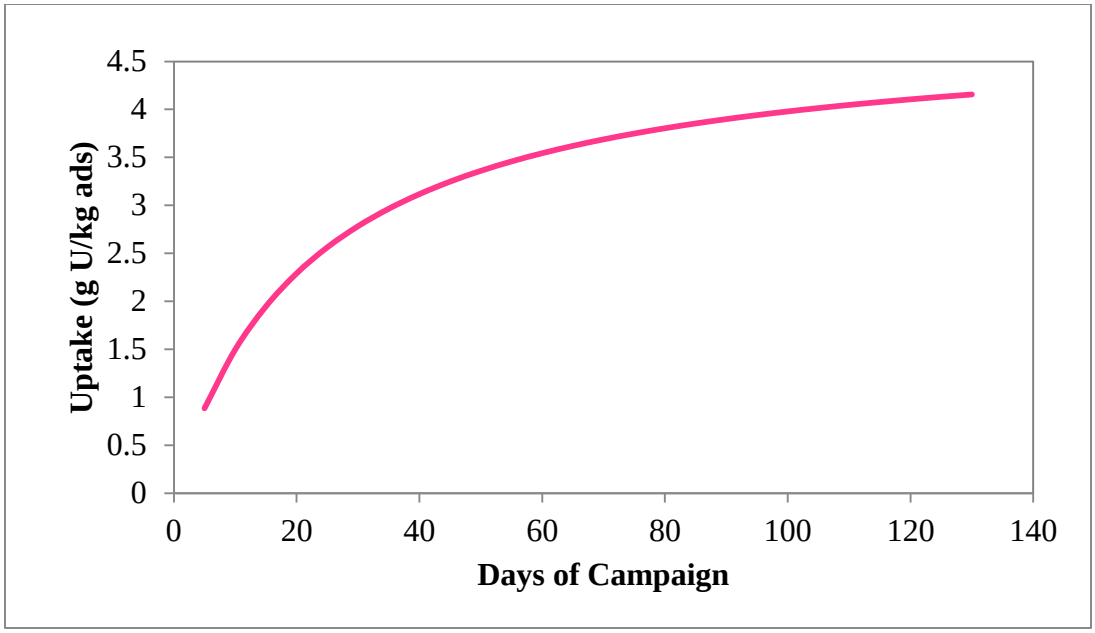

Figure 3.2: Adsorbent Uptake as a Function of Immersion Time

The length of campaign has the constraint of being greater than 0. Realistically, it can be expected that the length of campaign should not exceed the time it takes to reach 95% of the saturation capacity because beyond this point little gain will be realized by extended soaking times. If C_{max} is set to .95*B_{max} then the maximum campaign length for the reference AF1 case is 399 days.

TEMPERATURE

The relationship between uranium uptake of the ORNL adsorbent and ocean temperature was recently quantified and is here shown to have a significant effect on the final production cost. PNNL measured time series data for adsorbent uptake at three temperatures, allowing us to generalize the one-site ligand saturation model to predict adsorbent uptake as a function of temperature [19]. In order to carry out economic analyses it is necessary to relate the measured uptakes to both the temperature and immersion time.

Hence the time series measurements are used to create temperature dependent models for the kinetic parameters discussed earlier, β_{max} and K_D. Given the limited data, a linear regression was performed on all of the adsorbent types analyzed in the PNNL marine experiments. The relationships predicting β_{max} and K_D from temperature for the reference adsorbent type used in this analysis can be seen in Figure 3.3.

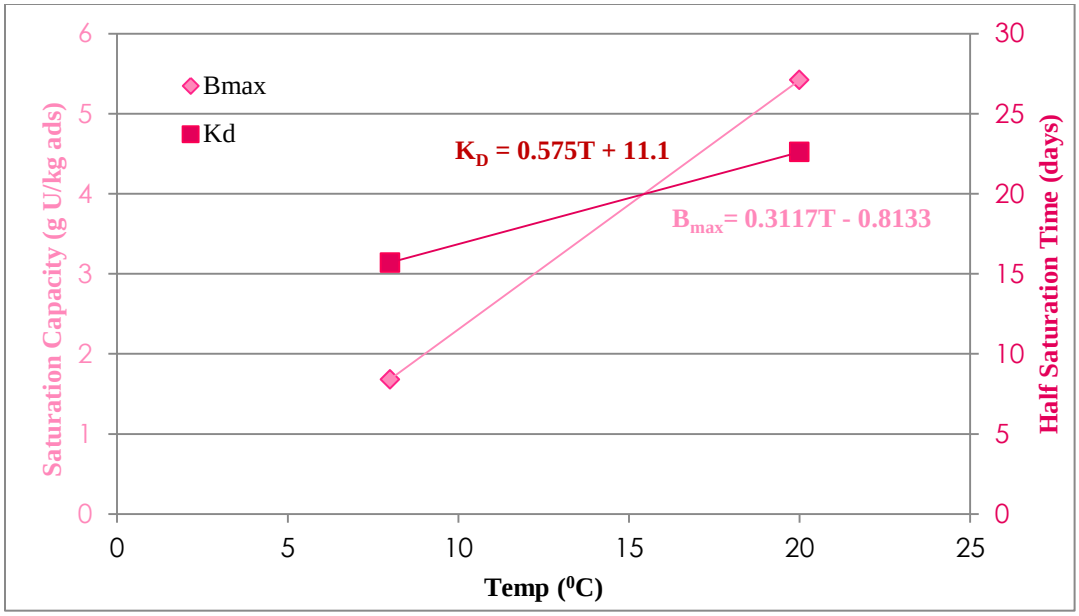

Figure 3.3: Temperature Dependence of Kinetic Parameters

These models for β_{max} and K_D are then placed back into the one site ligand saturation model discussed previously, Equation 3.21, to predict adsorbent uptake as a function of both time and temperature, $\boldsymbol{T}$, as seen below in Equation 3.22

$$C_{max} = \frac{(3112\boldsymbol{T} + 813) * t_i}{(0.575\boldsymbol{T} + 11.1) + t_i} \tag{3.22}$$

In most cases, adsorbents were analyzed at three temperatures, but in the case of the reference fiber, the data from the experiment containing the reference fiber at 32^{0}C

was not usable, leaving only the two lower temperature experiments. The use of this model is justified by the high R^2 values obtained by the same linear regression performed on the other fibers tested. Further verification of this model is assured by comparison to the empirical data in two ways. The time series uptake at any temperature as predicted by the regression model is consistently within 5% of the laboratory measured uptake. Even in the case of the missing data set, one point was recoverable and agreed with the model prediction to within 5%.

Degree of Grafting

The degree of grafting, g, is a measure of the addition of the amidoxime functional group to the HDPE backbone. It is a function of the weight of the ungrafted HDPE fibers,W_0, and the resulting weight of the grafted HDPE, W_g, and is defined according to Equation 3.23

$$g = \frac{W_g - W_0}{W_0} * 100\% \tag{3.23}$$

Increasing the ratio of ligand to backbone improves the adsorbents uptake but also increases the grafting chemical consumption and therefore operating costs of adsorbent production. Since the uranium bonds with the amidoxime, higher degrees of grafting generally lead to more available binding sites and a higher uranium capacity per mass of adsorbent. But experiments have demonstrated that once the grafting degree exceeds ca. 200-300%, the capacity of the adsorbent to take up uranium no longer increases [20]. It is hypothesized that the density of accessible binding sites reaches a plateau, and/or that diffusion of the uranium into the adsorbent begins to limit the uptake.

Empirical data has not yet been collected to determine the exact nature of the relationship between grafting degree and uptake or the limit beyond which uptake no

longer benefits from more grafting. Hence a notional relationship will be proposed between the actual capacity, *C*, at some degree of grafting and the maximum capacity, C_{max}, at a high degree of grafting. As mentioned, data has suggested that increasing the degree of grafting beyond 250% yields only marginal appreciation in capacity for uranium [21]. Therefore the feasible domain for capacity is bounded such that it cannot exceed the value achieved experimentally by 250% DOG. This presumed maximum comes from the assumption that eventually the increased ratio of ligand to backbone will yield no benefit due to physical interaction and/or competition between amidoxime sites. In the absence of experimental data, a hypothetical relation between g and C for $g <$ 250% is implemented by creating an inverted parabola passing through the point (g, C) = (0, 0) with a vertex at 250% DOG, seen mathematically below in Equation 3.24 and graphically in Figure 3.4.

$$C_{actual} = \begin{matrix} \frac{C_{max}}{\log(251)}\ if\ g > 250 \\ \log(250+1) * \frac{C_{max}}{\log(251)}\ if\ g > 250 \end{matrix} \tag{3.24}$$

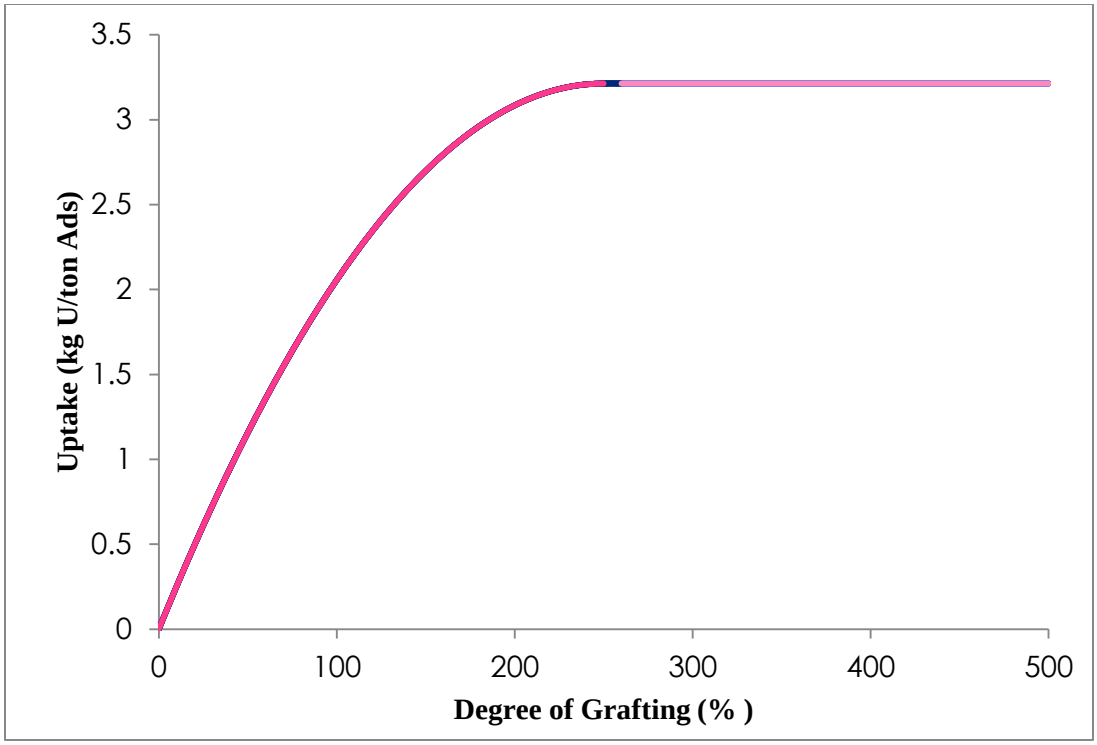

Figure 3.4: Uptake as a Function of Degree of Grafting

Although the PVC based adsorbent has demonstrated degrees of grafting above 1000% such high values have not been implemented on the reference HDPE fibers. Therefore in order to not risk compromising structural integrity, the maximum achievable degree of grafting will be set at 1000%. The DOG must also be greater than 0. If the algorithm sets the DOG to be less than or equal to 0 then the point is rejected and the DOG reset to 10% because below this value the uptake would be too low to be optimal.

It is understood that the DOG is by nature approximate and can vary between specimens of adsorbents. Hence a degree of grafting of exactly, say 250.000% cannot be guaranteed. But the degree of uncertainty and variability in the achieved DOG, relative to a given target DOG, has not yet been quantified. Therefore the DOG will be treated as

a real-valued number with no integer constraint in the optimization, but it is understood that there is uncertainty around the reality of attaining the predicted value exactly.

NUMBER OF USES

The number of times the adsorbent is used, N, also has an effect on the cost that is worth further examination as this parameter is easily manipulated. Although reusing the adsorbent circumvents the original production cost, the acidic chemical baths administered as part of the elution process degrade the uranium binding sites. In the base case the adsorbent suffers degradation, d, at a rate of 5% of the uptake achieved on the previous use [2]. This loss in uptake compounds with each use to have a non-trivial effect on the total uranium recovered by a unit mass of adsorbent over its lifetime, C_{tot}, as displayed in Equation 3.25

$$C_{tot} = \sum_{i=1}^{N} C * \left(1 - \frac{d}{100}\right)^{i-1} \tag{3.25}$$

After multiple uses the accumulated degradation eventually becomes high enough such that the marginal cost of another mooring, elution, and regeneration outweigh the marginal benefit. The cumulative lifetime uranium uptake for a unit mass of adsorbent as a function of number of uses is depicted in Figure 3.5.

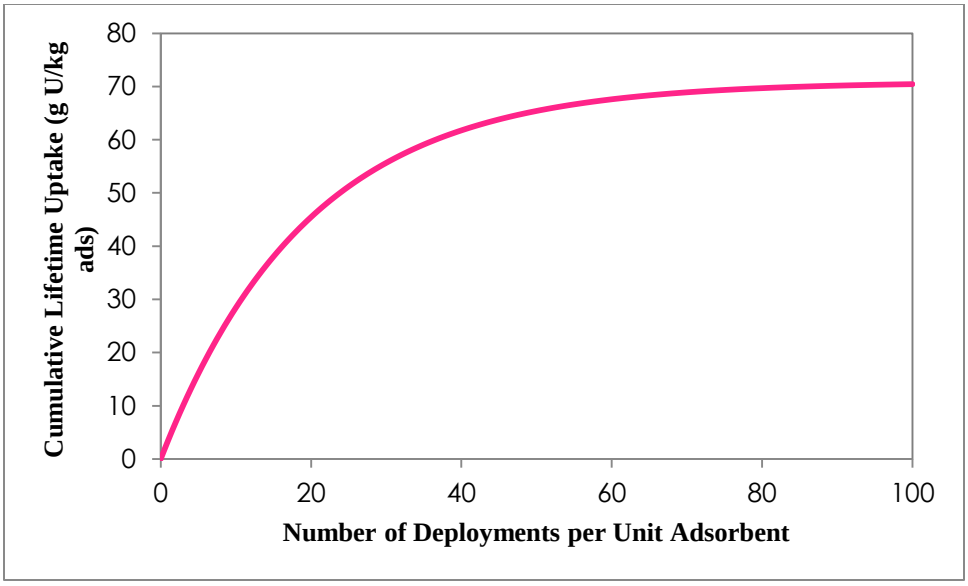

Figure 3.5: Total Uranium Uptake by Adsorbent over its Lifetime as a Function of Number of Uses

The only physical constraint on number of uses is that it must be a non-negative integer. Since the adsorbent suffers 5% loss in capacity with each re-use, it can be assumed that no more than 50 uses would be feasible.

BIOFOULING

The effects of biofouling on uranium uptake remain uncertain and are therefore neglected in the base case neglected. Although marine experiments have long resulted in discoloration of deployed adsorbent, the effect of biofouling on uptake has only recently been studied and is therefore largely uncertain. Due to the preliminary nature of existing data, significant extrapolation is used to create different hypothetical models in order to examine the potential impact biofouling could have on uranium cost. Intuition suggests that the degree of oceanic biofouling is proportional to at least two factors already otherwise incorporated to the cost analysis, length of campaign and temperature.

In order to clearly see the impacts of these two independent factors they will initially be analyzed individually before being combined. Biofouling will first be considered independent of both of these factors, to reflect the existing limited data. Secondly, the effects of biofouling will be assumed to be strictly a function of ocean temperature. Finally, effects of biofouling as a function of both ocean temperature and length of campaign will be explored.

Temperature and Time Independent Biofouling

It may be expected that the negative effects of marine organism activity on capacity would increase with time. Initial experimental data, however, has indicated that biofouling has little effect on rate of uptake, but simply decreases the uptake and capacity almost as soon as the adsorbent is placed in the water. It is hypothesized that this is a result of a difference in many orders of magnitude between the time scale of immersion times and marine organism reproduction time. Since the first data point is not taken until 7 days into soaking, it is possible that by this point the fibers have already reached their carrying capacity of microorganisms. If the net population is not changing with time this would lead to the observed effects of biofouling decreasing the maximum capacity and then having no further impacts. The correlation of biofouling effects and water temperature is also still undetermined. Therefore an initial analysis is conducted neglecting any such correlations.

The most recent data set regarding the effects of biofouling on uptake comes from experiments run at PNNL. Adsorbent fibers were exposed to filtered seawater and light for 56 days with their uranium uptakes periodically checked. The uptake of these fouled fibers is compared to the negative control, non-fouled fibers, to determine the effects on adsorbent uptake [22].

This time series data (Figure 3.6) is plotted below to show that the saturation capacity of the fouled fibers suffered a roughly 20% loss while the half saturation time was nearly unchanged, indicating no time dependence.

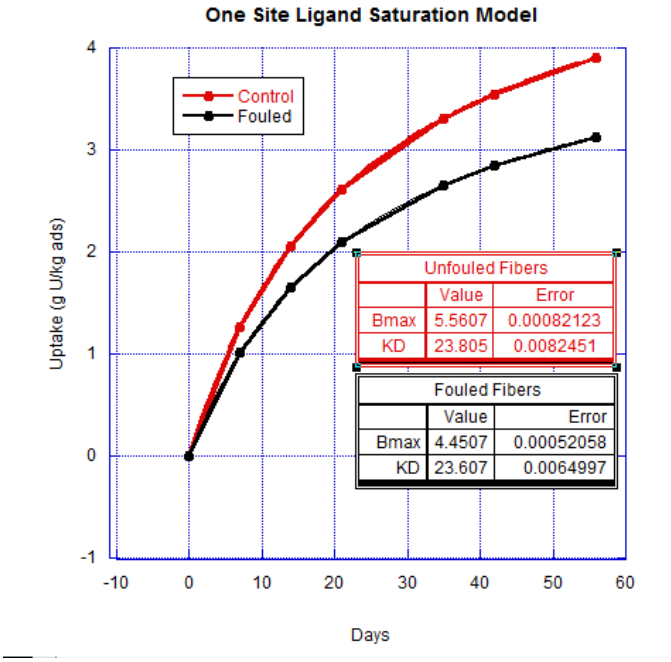

Figure 3.6: Initial Biofouling Data from PNNL

Although this data is limited in quantity and scope, as the most recent data set available its results are worth considering without any dependence on time or temperature. The effect of biofouling on B_{max} is incorporated to the base case and the optimal deployment conditions are found. Next a case hypothesizing a relationship between biofouling and temperature, and subsequently temperature and time, are considered.

Temperature Dependent, Time Independent Biofouling

Currently, the degree of biofouling is unrelated to the temperature of the seawater, although this is probably not indicative of reality. Therefore, a placeholder relationship is

derived and integrated to offset the unrealistic monotonic relationship between increasing temperature and uptake.

The recent experimental data (Figure 3.6) has indicated that biofouling has little effect on rate of uptake, rather simply decreases the maximum saturation capacity. There is a small difference, less than 1%, in the half saturation time, but this is believed to be in the noise as it has negligible effects on the uranium uptake for any given length of campaign. Regardless of the significance of this change in K_D, the decreased uptake caused by a lower saturation capacity is likely to alter the optimal conditions and therefore worth exploring.

While the uranium complexation with amidoxime favors warmer waters, it is likely that a competing feedback of increased biofouling also exists at these elevated temperatures. Beyond visual inspection, though, no empirical correlation between loss in uptake and presence of microorganisms has yet been obtained. Therefore, in order to quantify this relationship, the literature is reviewed for correlations relating organism specific growth rate, in units of inverse time, to temperature. A general formula relating heterotrophic bacterial specific growth rate, G in units of inverse time, and ocean temperature, T, found in the literature, and seen in Equation 3.26, is thus used to correlate the effects of biofouling to water temperature [23].

$$log(G) = -1.54 + 0.052\boldsymbol{T} \tag{3.26}$$

Since previous experiments have shown that temperature has been seen to affect the adsorbent capacity but not the kinetics, this temperature dependent biofouling is applied to the saturation capacity. No suitable correlation between growth and

temperature which might be applicable to fouling of the adsorbent surface was found. Therefore, the single known data set, a 20% decrease in B_{max} at 20^0C, is used to normalize all other growth rates to a loss in adsorbent capacity.

The effect of biofouling on B_{max} is computed using a ratio of the growth rate at any given temperature, T, relative to the growth rate at 20^0C, and then scaled by the reference 20% loss. This temperature dependent loss is shown mathematically below in Equation 3.27. Figure 3.7 provides a graphical example of this effect by showing the uptake realized by a unit mass of adsorbent as a function of temperature for a 60 day campaign.

$$B_{max}(T) = B_{max}\left(T_{no\ fouling}\right) * \left(1 - \frac{10^{-1.54+.052*\boldsymbol{T}}}{10^{-1.54+.052*\boldsymbol{20}}} * 20\%\right) \tag{3.27}$$

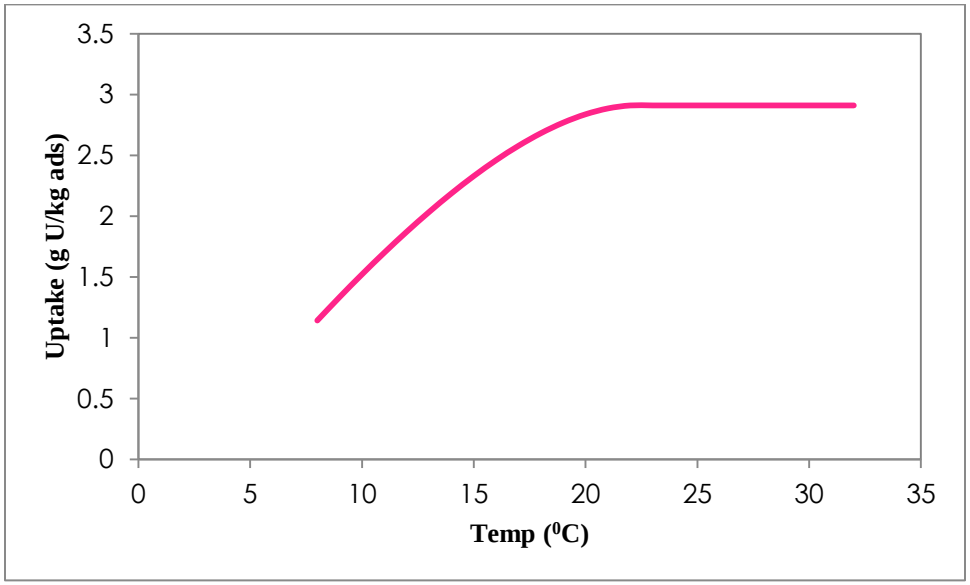

Figure 3.7: Uptake as a Function of Temperature for the case of Temperature Dependent, Time Indented Biofouling

In modeling the effects of biofouling this temperature dependent reduction of capacity is applied. Existing data does not indicate that biofouling is a function of time

and there is little reason to believe that that the kinetics would be a function of temperature. Therefore, the half saturation time, K_D, has no dependence on temperature. Intuition does suggest however that the effects of biofouling would increase with longer soaking times, but this is not supported by the preliminary data. Nonetheless it is worth exploring the hypothesis that biofouling is in fact dependent on time in addition to temperature

Temperature and Time Dependent Biofouling

Since no data currently exists to suggest a relationship between length of campaign, t_i, and loss due to biofouling, a linear model is drawn from the existing data. For the purposes of this hypothesis, it is assumed that the effects of biofouling begin upon the adsorbents' immediate contact with water and increase linearly, passing through the point (56 days, 20% loss in uptake), which comes from the data displayed in Figure 3.6 above. This decreased uptake relative to the unfouled fibers is calculated in Equation 3.28 below, for any given temperature.

$$uptake = uptake(no\ fouling) * (1 - 0.353t_i) \tag{3.28}$$

To relate the fouling back to temperature, the specific growth rate as a function of temperature is again used. The loss predicted at a given length of campaign by Equation 3.28 above is multiplied by the temperature dependent loss calculated in Equation 3.27. These combined effects of biofouling on uptake can be seen in Equation 3.29 and Figure 3.8 below.

$$uptake(T, t_i) = uptake\left(T_{no\ fouling}, t_{i,no\ fouling}\right) * \left(1 - 0.353 t_i * \left(\frac{10^{-1.54+.052*\boldsymbol{T}}}{10^{-1.54+.052*\boldsymbol{20}}}\right)\right) \quad (3.29)$$

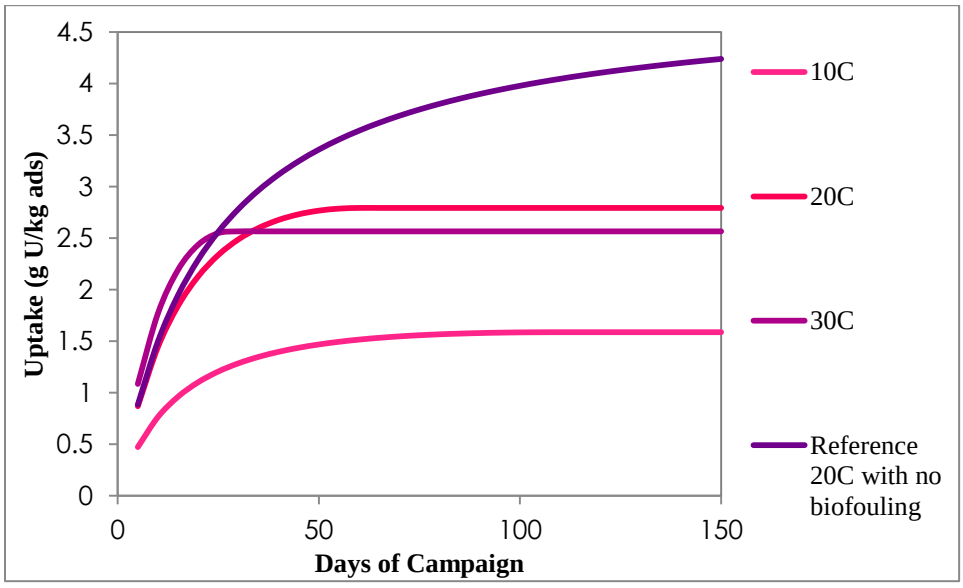

Figure 3.8: Uptake as a Function of Temperature for the case of Temperature and Time Dependent Biofouling

It is worth noting that for some water temperature and immersion time combinations the uptake begins to decrease. This however is non-physical, so the point at which this happens is considered the point of maximum biofouling and beyond that point the uptake is assumed constant.

BICARBONATE ELUTION

The current acidic elution process leads to degradation of the adsorbent with subsequent reuse. Ongoing research at the University of Idaho has indicated that this degradation may be mitigated or removed altogether by the replacement of a bicarbonate

solution [24]. Although there are still uncertainties surrounding this process, it is still an interesting case study to investigate.

The process under investigation involves the use of a potassium bicarbonate solution to selectively remove uranium off the adsorbent. Preliminary studies have shown that this method provides the benefit of uranium selectivity along with little to no adsorbent degradation. Additionally, since a basic solution has replaced the previously used acids, the adsorbent no longer needs to be regenerated with alkaline solution. The elimination of this step provides a significant cost savings through the reduction of chemical consumptions.

The benefits of reduced degradation and increased selectivity following from use the basic solution, while potentially considerable, are not well-quantified and remain subject to significant uncertainty. All of the experiments carried out thus far have utilized uranium doped solution. Therefore the high uptake achieved by subsequent immersions may not necessarily be achievable in real seawater. Similarly, the removal of by-products may present a bigger issue in reality than on the bench top. Since the potassium bicarbonate has such a high affinity for uranium, it does not remove other metals off the adsorbent. In high concentrations of uranium Le Chatellier's principle will push the uranium onto the adsorbent in place of other metals, but in real seawater this is not likely to be the case.

In order to reflect the uncertainty surrounding this method a sensitivity analyses to cost as a function of degradation rate is examined. The developers claim to have observed degradation rates below 1% per re-use. Conversely, the failure to remove unwanted metals may lead to a loss in uptake due to the occupation of binding sites. Therefore the true degradation is largely unknown and the sensitivity analysis will consider degradation rates ranging from 1-15% loss in uptake per re-use.

Cost Minimization

Brute Force Calculation

To validate the implementation of the chosen algorithm, a method of benchmarking the results must be determined. The true minimum could be found by through a brute force calculation of all of the possible combinations of parameter values. Since the degree of grafting and days of immersion are not being rounded and subsequently have an infinite number of possible values, this can only be done to within a finite interval which is defined by the discretization of these variables in the brute-force sweep.

Although the length of campaign is a continuous variable, for the simplification of a brute force calculation, the soaking time is only considered in increments of five days. Similarly, the degree of grafting is only allowed to be multiples of ten.

Calculating the cost for all of the possible combinations of the parameter values given these restrictions produces a minimum cost of $548.9; the decision variable values producing this cost are show in table 3.2

Table 3.2: Brute Force Verification Optimal Results

Parameter	Value
Cost	$549.9/kg U
Length of Campaign	60 days
Number of Uses	15 uses
Degree of Grafting	240%

Although this cost is not precisely the minimum given the discretization of the campaign length and DOG, it gives insight to the region containing the minimum. If the algorithm selected does not return a cost below this value, then it is obviously not converging on the global minimum. Figure 3.9 below shows cost as a function of degree

of grafting and length of campaign if the adsorbent is used 15 times, which is the area of the feasible region in which the algorithm should be converging.

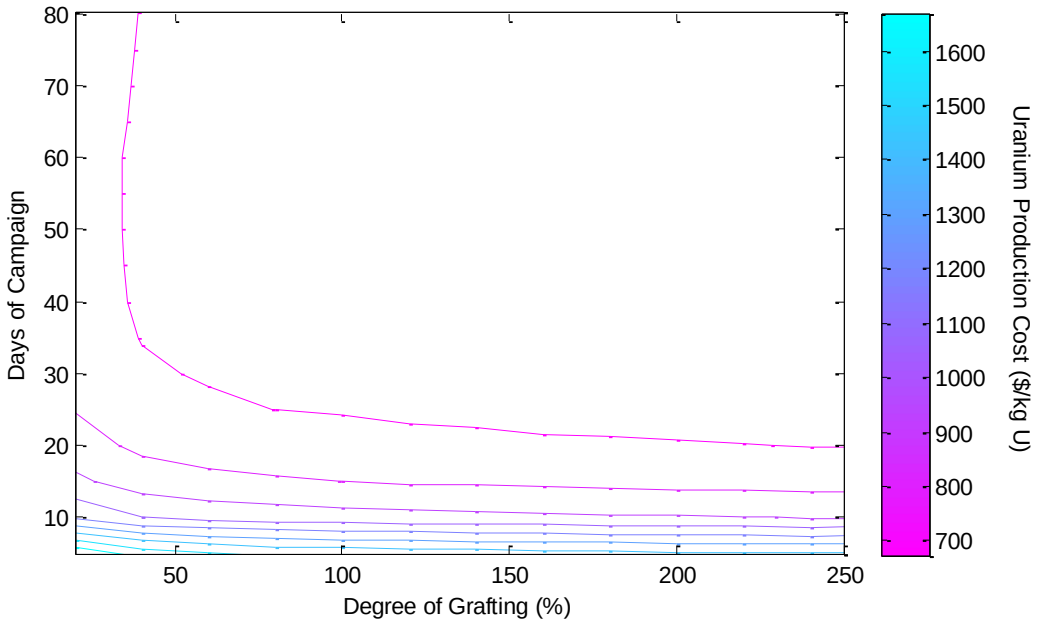

Figure 3.9: Region of Minimum Cost as Determined by Coarse Brute Force Calculation

Having identified the area of the minimum, the brute force calculation is repeated over a smaller space using finer intervals. Based on the optimal conditions found from the first sweep, a new narrower range is chosen for each decision. The discretization for the days of campaign is decreased to intervals of two days and the DOG in intervals of 10%. The results of this brute force calculation are displayed in Figures 3.10-3.12 below.

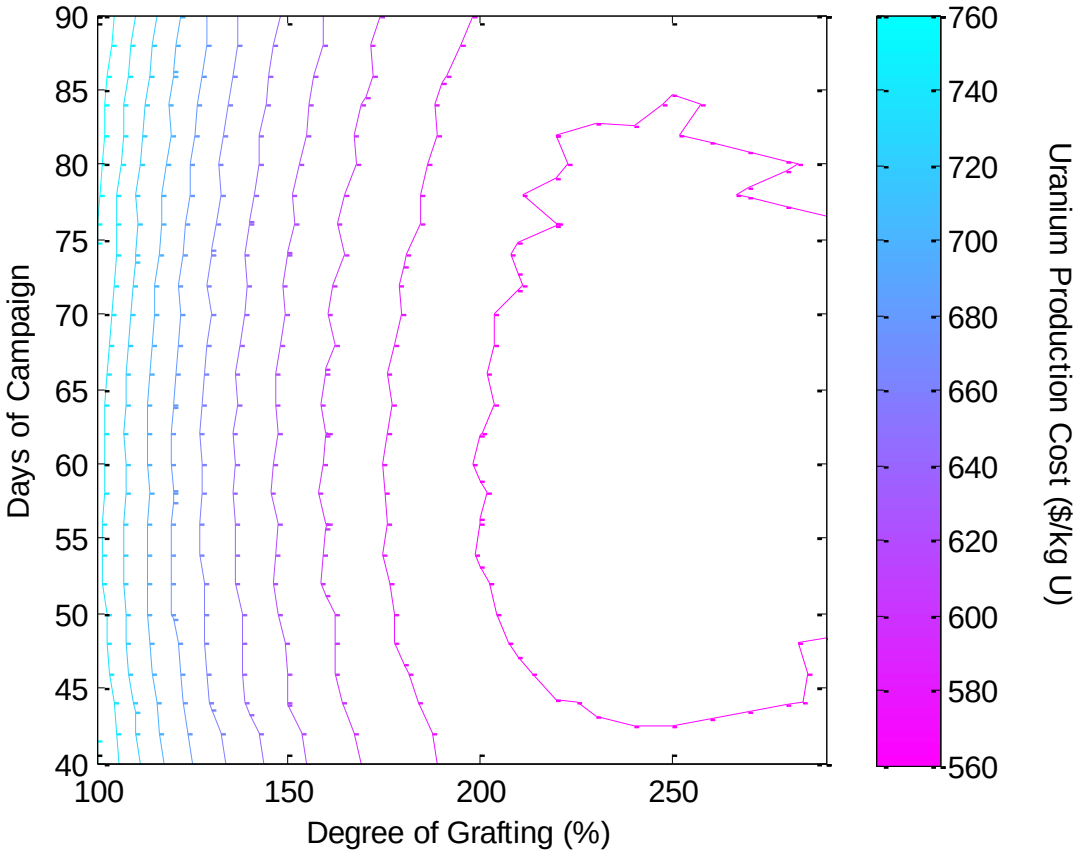

Figure 3.10: Region of Minimum Cost for 14 Uses as Determined by Finer Brute Force Calculation

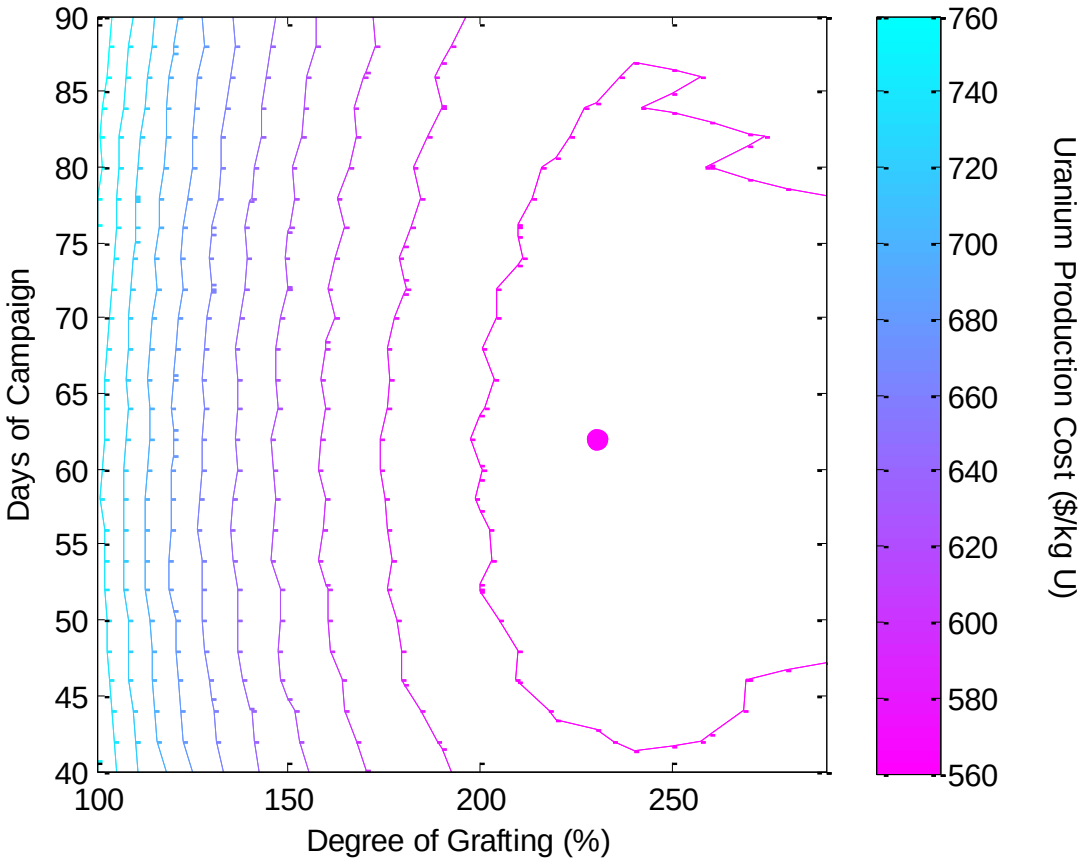

Figure 3.11: Region of Minimum Cost for 15 Uses as Determined by Finer Brute Force Calculation

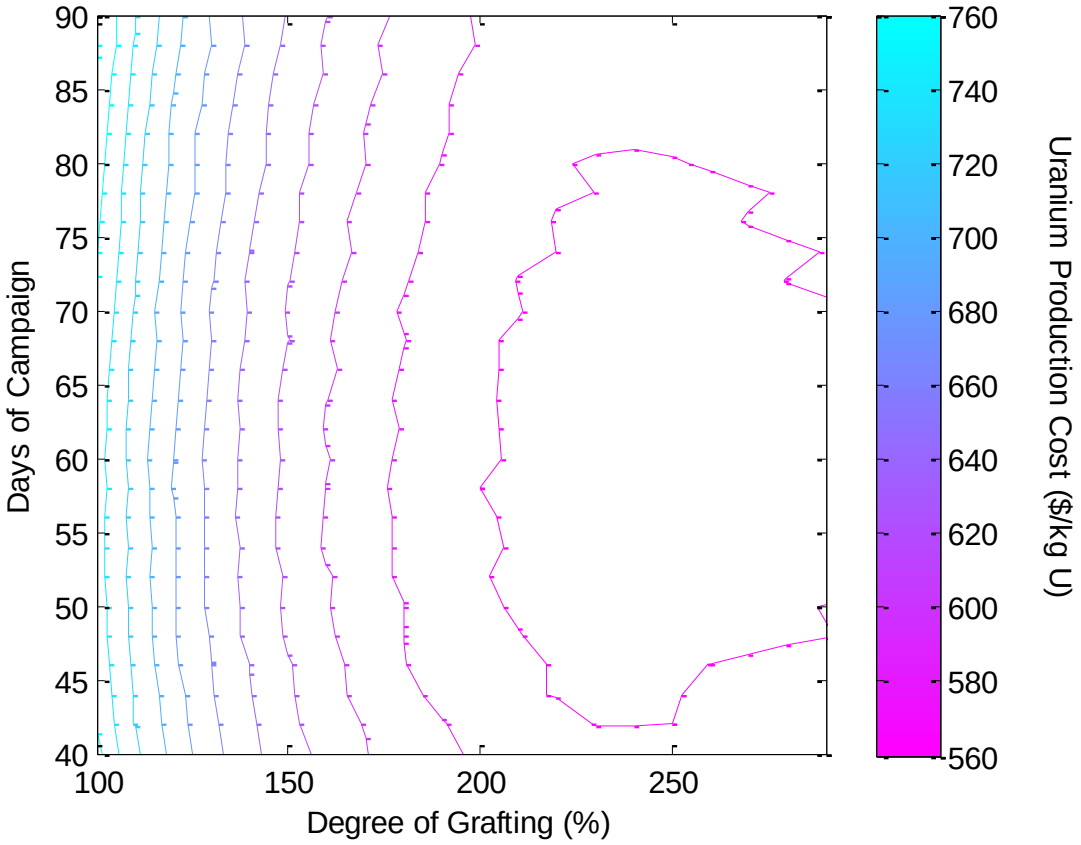

Figure 3.12: Region of Minimum Cost for 16 Uses as Determined by Finer Brute Force Calculation

It might be expected that the contours on the above figures would be smooth. The irregularities arise due to changes in the deployment system design that occur within the black box cost model in response to changes in adsorbent capacity, length of campaign, and other parameters. These manifest as small discontinuities in the cost between neighboring points whenever an integer constraint becomes active inside the black box cost model. Integer constrains in the model include the number of work boats required to service the adsorbent field along with the number of chains used to moor adsorbent to the ocean floor. Whenever one of these values is changed by an integer amount, the

irregularities, which are especially visible near the shallow minimum, result. These effects are less visible elsewhere where the cost gradient is steeper, as the variation due to integer constraints is generally on the order of $1-2 and therefore only become visible in regions where the cost is nearly flat.

From this calculation the minimum is determined to be $546.3 as marked on Figure 3.11. The deployment conditions required to obtain this value are shown in Table 3.3. Therefore the results of the minimization algorithm will be verified by producing values in this region with a minimum at or more likely below this cost.

Table 3.3: Optimal Results from Brute Force Verification using Finer Intervals

Parameter	Value
Cost	$546.3/kg U
Length of Campaign	62 days
Number of Uses	14 uses
Degree of Grafting	230%

ALGORITHM IMPLEMENTATION

As mentioned this optimization problem was first attempted via Newton's method with finite differencing used to estimate both the Jacobian and Hessian. This method would often fail to converge as the step size, notably in the degree of grafting, was so large that it would push the answer toward the bounds of the feasible region. This is presumably due to the zero-valued slope of uptake with respect to degree of grafting near the shallow optimum. To combat this issue a Armijo-Goldstein condition was used to find an appropriate step size.

The Goldstein condition used is a backtracking line search methods of determining an appropriate step size in order to make significant progress in minimizing

the objective function without moving too far in the direction of descent. The step direction found by Newton's method is used in combination with this pseudo minimization to reduce the objective function at the new location relative to the previous point. The step size, σ, is initialized as unity, i.e. a standard Newton move (Equation 3.30), and iteratively backtracked down to a lower value.

$$x_{i+1} = x_i - \sigma \frac{J_i}{H_i} \tag{3.30}$$

This decrease in step size continues until the difference between the objective function value corresponding to the kth step size is lower than the objective function value from the previous Newton iteration, $f(x^{i-1})$, is below a predetermined threshold.

$$f\left(x^{i-1}\right) - f(x^{i-1} + \sigma_k \frac{J_i}{H_i}) \geq \sigma_k \mu J_i \tag{3.31}$$

The threshold is a function of the local slope determined by the Newton iteration, *J*, and a constant μ which must be between 0 and 1 and is often chosen to be 0.5. If this condition is not met the step size is iteratively lowered by a factor of 0.5 and incrementing *k* until an appropriate step size is achieved [25].

While this was successful in avoiding an infinite loop of continually resetting the domain to be with in the feasible region, it was not successful in consistently finding the minimum value of the objective function. It was found that the Hessian approximated via this method is not assured to be positive definite for every iteration. Therefore the algorithm sometimes moves in a direction of increasing objective function value. Hence, the decision was made to make use of a different quasi-Newton method, the Broyden-Fletcher-Goldfarb-Shanno (BFGS) method [26].

The BFGS method is a quasi-Newton method that updates the Hessian based on previously calculated estimates of the Hessian, thereby circumventing the need for second derivatives. Additionally, the BFGS method ensures the Hessian will be positive definite, whereas the finite differencing approach used in the previous attempt did not.

Since the BFGS updates the estimate of the Hessian with each move and the initial move requires a Hessian, the Hessian is initialized as the identity matrix as this guarantees positive definiteness. This appears to be problematic in the degree of grafting domain due to an integer constraint put on the DOG. The slope of the cost with respect to the degree of grafting is quite small, especially in regions of interest between 230-250%. When the Hessian is the identity, or very close, then the delta value calculated for the DOG is often below .5 and would thus round down to 0 so little progress was made. The integer constraint proved too problematic for the minimization of this shallow optimum. Therefore the decision was made to move away from Newton's method and the integer constraint on DOG all together. Initially it was assumed that due to a lack of accuracy in achieving a uniform DOG amongst all adsorbent samples should be combatted by rounding the DOG to discrete integers. Later however it was decided that a better approach would be to allow the variable to remain continuous, with the understanding that the values attained in practice would be presumably distributed around the mean value predicted by the optimization.

Even with the removal of the integer constraints, aside from the constraint on number of uses which is physical in nature, the BFGS method was unsuccessful. The minimum identified by the method was seen to be dependent on the size of the interval used to approximate the slope and the starting point of the algorithm. While tightening the convergence criteria did result in improvements, as the criterion became increasingly strict, the time required to run the minimization also increased. It has already been

mentioned that the region of the minimum cost is shallow, but this trial and error has indicated that it is in fact so shallow that Newton's method, with or without the BFGS variation, is not an appropriate algorithm.

One disadvantage of both variations of the Newton's methods used here comes from the Jacobian and sometimes Hessian estimations. As mentioned in the literature review there is additional error introduced when using finite differencing in place of a true derivative. But in addition to this issue is the need to calculate additional objective function values, slowing down the process. This is particularly unfavorable in the case of uranium from seawater cost minimization where the black box calculation of the uranium production cost is the most time consuming step. The Newton's method coupled with central differencing described in the literature review requires two objective function calculations for the estimation of the Jacobian and four for the Hessian in each iteration. While the BFGS method removes the necessity of four calculations required for the Hessian, two uranium production costs still need to be calculated before the new point can be determined and the new cost calculated. Therefore, in the interest of computational time algorithms tailored for black box optimization will be explored.

Finally a true derivative free optimization method found in the literature was attempted, the Nelder-Mead simplex method for non-linear optimization. Although this direct search method is designed for unconstrained optimization, the constraints will be implemented through the logic embedded in the code. This is done by forcing any non-feasible decision variables back to their boundary values and continuing the algorithm as usual. This is presumed to be a sufficient fix because it is unlikely that the optimal values of decision variables will be at or near the boundaries of the feasible region. In fact if this does turn out to be the case, then a different parameter should be considered for optimization as there is little insight to be gained if the optimal objective function is

achieved pushing a given parameter to the edge of the range of value it is allowed to take on.

As mentioned previously, the method follows the movement of a simplex through the parameter space until it converges to a small enough volume. Given that the current problem formulation deals with three variables (days of campaign, number of uses, and degree of grafting) the simplex utilized is a tetrahedron. With each iteration the simplex moves in such a way that the vertex corresponding to the highest value objective function is replaced with a new set of points yielding a lower objective function. For this analysis the coefficient values, are based off of commonly accepted values seen in Table 3.4 [27].

Table 3.4: Coefficient Values used in Nelder-Mead Simplex Algorithm

Simplex Move Coefficient Values		
Coefficient Type	**Symbol**	**Value**
Reflection Coefficient	α	1
Expansion Coefficient	γ	2
Contraction Coefficient	β	0.5
Shrink Coefficient	δ	0.5
Convergence Criteria for Standard Error	ε	$1x10^{-10}$

The appropriate convergence criterion is selected by iteratively running the algorithm with increasingly smaller epsilon values, where ε is calculated as the standard error of the uranium production costs, uc_u, of each vertex of the current simplex as seen in Equation 3.32.

$$\varepsilon = \sqrt{\sum_{j=1}^{n+1} \frac{\left(uc_{u,j} - \overline{uc_u}\right)^2}{n}} \tag{3.32}$$

The results of these trials are shown in Table 3.5. Also in the table is the approximate minimum cost found by a "brute-force" parameter sweep. The algorithm quickly finds and improves upon this minimum. Increasing the convergence criteria beyond $1x10^{-10}$ offers little to no decrease in the minimum cost returned by the algorithm but does increase the required time. Below this value the computed minima show slight fluctuations since the minimum is very shallow. The fluctuations however are on the order of tens of cents and are therefore negligible. These fluctuations may arise due to the aforementioned discrete values used in the cost calculation. The existence of discrete values gives rise to numerous local minima that differ from the global minimum by a very small amount. And since sensitivity analyses will be conducted requiring the algorithm to be run many times, this seemingly small increase in time will have a non-negligible effect in the total run time. Therefore, an epsilon value of $1x10^{-10}$ is considered sufficient.

Table 3.5: Resulting Optima used in Convergence Criteria Determination

ε	Number of Iterations	Time (seconds)	Minimum Cost ($/kg U)	Optimal Days	Optimal Number of Uses	Optimal DOG (%)
Brute Force	-	-	546.3	62	14	230
$1E^{-2}$	9,756	1,002	547.4	67.6	13	232.6
$1E^{-4}$	13,592	1,426	546.2	62.2	14	234.1
$1E^{-6}$	18,024	2,208	546.2	65.9	14	240.5
$1E^{-8}$	19,444	2,112	546.0	59.2	14	243.0
$1E^{-10}$	20,956	2,547	545.7	58.9	14	235.5
$1E^{-15}$	21,164	2,598	545.9	55.7	14	241.3
$1E^{-20}$	22,216	2,785	545.7	58.9	14	235.1

The initial simplex is generated by randomly manipulating the user specified starting point to produce three additional points using Matlab's built in random number

generator. This unique stochastic addition to an otherwise deterministic algorithm was implemented in order to remove starting point dependence and increase the chances of converging on a global as opposed to local minima. A standard simplex algorithm described in the lit review is used until the tetrahedron collapses to roughly a single point [9]. In addition to the convergence criteria discussed above derived from the standard method, a stationary iteration, i.e. having all the same vertices as the previous iteration, also ceases the algorithm. This predicted minimum is recorded and the process initialized again by generating three random points around this new minimum. To avoid convergence on a local minimum, the algorithm is repeated until the same minimum is output 10 times in a row. The selection of 10 local restarts comes both from the literature and the observation that the predicted minimum may change after only a few runs [28].

Unique to this analysis is the integer constraint on the number of uses of a unit mass of adsorbent. The algorithm generally returns non-integer values for this decision variable, but the integer constraint must be imposed. Therefore this minimization deals with this issue by rounding the continuous value outputted by the standard algorithm both up and down to end up with two possibilities for number or uses. Both of these use values are input to the black box cost model with all other decision variable values remaining constant. The number of uses resulting in the lower of the two costs is the one selected to continue the algorithm.

RESULTS

Individual Case Optima

The chemical and engineering processes associated with the braided adsorbent system are evolving with time. Ongoing changes to the technology make it impossible to define a reference set of parameters that accurately reflects those most likely to be adopted upon industrial scale up. However, in order to clearly distinguish economic impacts of important cost drivers and provide a starting point for optimization, it is necessary to consider a single scenario yielding an illustrative cost. For the purposes of this analysis such a base case yielding a uranium production cost of $616/kg is defined according to Table 4.1 below. The values in this case come from ORNL laboratory data, previous deployments by the JAEA, and previous cost estimates [2], [15], [21], and [29]. This case is used for illustrative purposes only and is not meant to be interpreted as a reference case.

Table 4.1: Base Case Description

Parameter	Illustrative Value	Unit
Illustrative Uranium Production Cost	**616**	**$/kg U**
Degree of Grafting	250	%
Number of Uses	6	Deployments
Degradation Rate	5	% loss per re-use
Length of Campaign	60	days
Ocean Temperature	20	^{0}C
Biofouling	Neglected	

BASE CASE OPTIMUM

The first case to be optimized is the use of the illustrative reference case as the initial guess. Running the optimization returns a cost of $545.7/kg U, an 11% decrease from the original $616.

The implementation of the minimization algorithm can be verified by comparing the result it returns with a brute force pseudo-minimization of the same case. Table 4.2 shows that the Nelder-Mead algorithm returns a uranium production cost value that is marginally lower than that predicted by the brute force calculation. This is unsurprising as the brute force calculation can only calculate the cost at selected discrete values of each cost-driving variable. In Table 4.2 the results of the coarse-interval brute force calculation run earlier are included along with a more finely meshed sweep where DOG and days of campaign are intervals of one integer unit. The optimal values for the optimal length of campaign and DOG broadly agree across all three optimization approaches.

Table 4.2: Optimized reference case: comparison of brute force and Nelder-mead algorithm minimization results

Parameter	Brute Force: Coarse Interval	Brute Force: Fine Intervals	Nelder-Mead Algorithm
Minimized Cost	$546.3/kg U	$545.7/kg U	$545.7/kg U
Length of Campaign	62 days	59 days	58.9 days
Number of Uses	14 uses	14 uses	14 uses
Degree of Grafting	230%	238%	235.2%

BIOFOULING OPTIMUM

Temperature and Time Independent Biofouling

The first biofouling scenario considered is one in which biofouling is independent of time and temperature. As expected the lowest achievable cost of uranium production is higher than the base case, which was free of biofouling, and comes in at $660.9/kg U. The optimal conditions differ from that of the reference case as seen in Table 4.3. A very notable difference exists in the optimal DOG, which is higher than that of the base case. With a lower saturation capacity, and thus realized uptake, higher degrees of grafting are favored since the increase in uptake outweighs the increased chemical costs. Increasing the DOG appears to be the most economical way to increase the uranium recovery as the length of campaign is lowered while the number of uses stays the same. Since the uptake is 20% lower than the reference case the marginal increase in uranium obtained by extending the immersion time is also decreased.

Table 4.3: Temperature and Time Independent Biofouling Optimum

Parameter	Value
Cost	$660.3/kg U
Length of Campaign	56.4 days
Number of Uses	14 uses
Degree of Grafting	242.1%

Temperature Dependent, Time Independent Biofouling

The second scenario hypothesizes the effects of biofouling to be temperature dependent. The point at which increasing uptake and biofouling due to increasing temperature are offset by each other can be seen in the optimal conditions in Table 4.4 to yield a cost of $644.1/kg U. It is worth noting that the optimal temperature is not 30^0C

but close to 20^0C in this case. At 30^0C although the uptake is greatest, the heightened biofouling causes a roughly 60% loss in uptake, as compared to the 20% in the reference 20^0C case.

Table 4.4: Temperature Dependent, Time Independent Biofouling Optimum

Parameter	Value
Cost	$644.1
Length of Campaign	63.5 days
Number of Uses	13 uses
Degree of Grafting	241.9 %
Temperature	22.5 ^{0}C
Loss in Uptake	26.8%

Temperature and Time Dependent Biofouling

The optimal cost in this case is $597.2 (Table 4.5). This is lower than the time independent case because at the optimal length of campaign, which is found to just 34 days, the loss due to biofouling is lower than the case above. Under the time-dependent fouling model assumed for this study, it becomes optimal to favor very short campaigns where the adsorbent is withdrawn before biofouling really starts to have a significant effect on uptake. Note that if this scenario proves to resemble realistic biofouling behavior, then the cost benefits of improving the kinetic behavior of the adsorbent will markedly increase.

Table 4.5: Temperature and Time Dependent Biofouling Optimum

Parameter	Value
Cost	$597.2/kg U
Length of Campaign	32.1 days
Number of Uses	15 uses
Degree of Grafting	228.1 %
Temperature	25.5 ^{0}C
Loss in Uptake	22.0%

BICARBONATE OPTIMUM

If the bicarbonate elution can be perfected and adopted uranium production cost would decrease by about 20% to be $445.2, assuming the degradation rate is identical to the acidic alternative (5%). The optimal set of conditions is substantially different from the reference case, though-notably, the number of uses changes. Not surprisingly, the optimal number of uses is higher because there is no costly regeneration required for each re-use. If the degradation proves to be lower than 5% then the minimum cost can be reduced even further as the number of uses would increase. The minimum uranium production costs and their associated optimal deployment scenarios for a variety of degradation rates are displayed in Table 4.6 below.

Table 4.6: Bicarbonate Elution Sensitivity Optima

Degradation:	1%	5%	10%	15%
Minimum Cost	$322.2	$445.2	$550.9	$635.3
Length of Campaign	46.4 days	50.7 days	56.2 days	59.1 days
Number of Uses	29 uses	17 uses	10 uses	8 uses
Degree of Grafting	248.8%	245.6 %	242.3%	239.3%

Whether the bicarbonate elution process is more favorable than the acidic depends upon many factors. Therefore an additional optimization tool built into the code considers the elution process as a binary variable. In this case, the user is able to input a degradation rate realized by each of the processes. The algorithm first finds the minimum cost achievable by the acidic elution process, with the user specified acidic degradation rate. Then it again minimizes the cost given that bicarbonate elution is used with its user specified unique degradation rate. The two minima are then compared and the lowest is selected. The output of an example run of this feature can be seen in the

Figure 4.1 below with the detailed results in Table 4.7. In this example run, the degradation rate for bicarbonate is assumed to be 9% because data from Table 4.6 indicates this loss rate may be near the tipping point at which the acidic process becomes advantageous.

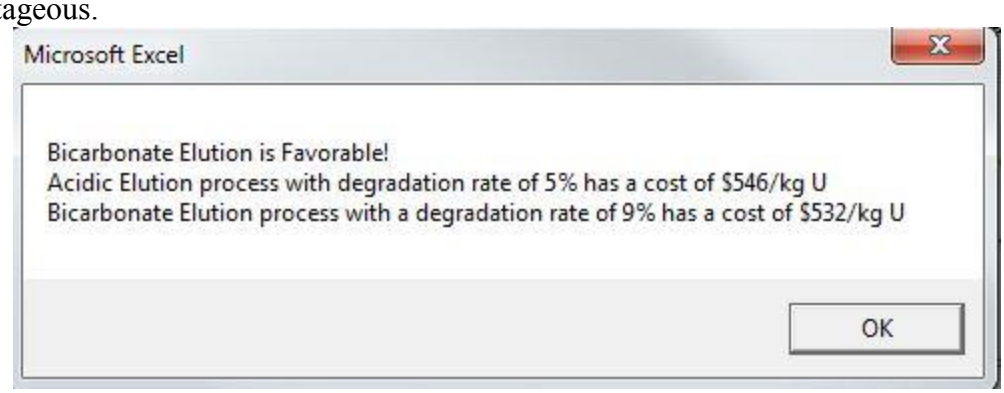

Figure 4.1: Output of Binary Elution Optimization

Table 4.7: Results of Binary Elution Optimization

Parameter	Acidic Eltuion	Bicarbonate Elution
Degradation	5%	9%
Minimum Cost	$545.7/kg U	$532.3/kg U
Length of Campaign	58.9 days	56.4 days
Number of Uses	14 uses	11 uses
Degree of Grafting	235.2%	246.3%

The contour plot in Figure 4.2 shows the minimum cost achievable for a range of degradation rates. The black diagonal line shows the region in which the desired elution process changes. Below the black line acidic elution is favorable while above the black line the bicarbonate process is advantageous. Since the acidic elution process requires the costly alkaline regeneration step it only becomes favorable when the degradation rate caused by the bicarbonate elution process is quite high. If the bicarbonate elution process proves to have a very low degradation rate then substantial uranium production cost

would result. Conversely, if the acidic degradation rate proves to be higher than expected, then the cost of uranium from seawater will increase.

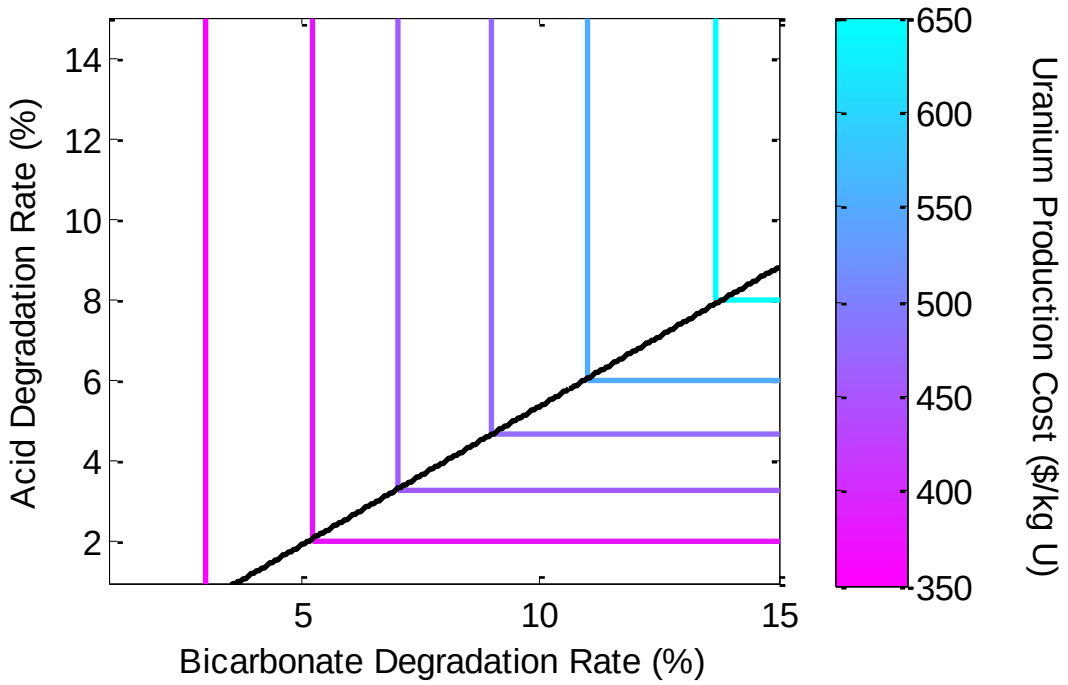

Figure 4.2: Uranium Production Cost as a Function of Acidic and Bicarbonate Elution Process Degradation Rates

Sensitivity Analyses

The technology used in the recovery of uranium from seawater is constantly evolving. Additionally, each cost input and adsorbent characteristic has its own uncertainty. Therefore, many elements affecting the final uranium production cost are subject to considerable uncertainty as well. In anticipation of potential changes and to provide intuition for determining optimal conditions sensitivity analyses to various decision variables and cost inputs are conducted.

INPUT COST VARIATION

The first sensitivity explores the effects of changing the input costs in the reference scenario of neglected biofouling. Both the deployment cost for a unit mass of adsorbent and the price of the grafting chemicals are altered. To create the upcoming sensitivity plots, the optimization is run many times, with each run multiplying the base case deployment and grafting chemical costs by a factor ranging between 0.5 and 1.5. The resulting optimal production cost as a function of these parameters is plotted in Figure 4.3. Each (deployment cost, grafting cost) point in Figure 4.3 is associated with a unique optimum adsorbent configuration and deployment strategy. Figures 4.4-6 plot the optimal campaign length, number of uses of the adsorbent, and grafting degree that gives rise to the minimized cost surface of Figure 4.3.

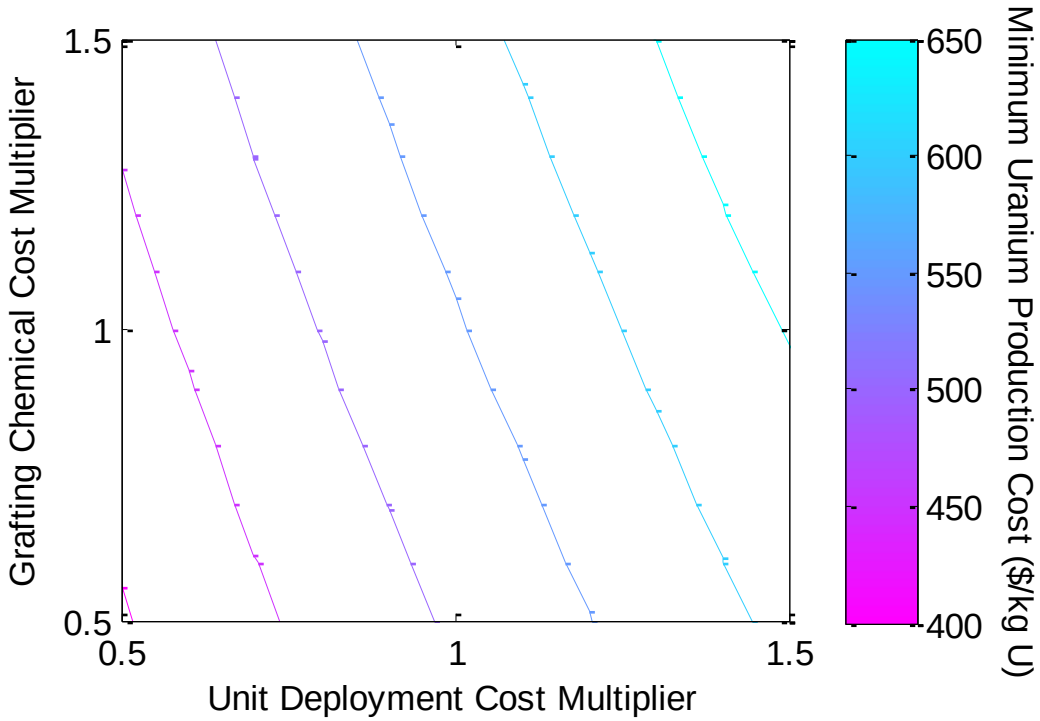

Figure 4.3: Minimized Uranium Production Cost as a Function of Deployment and Grafting Chemical Cost Multipliers

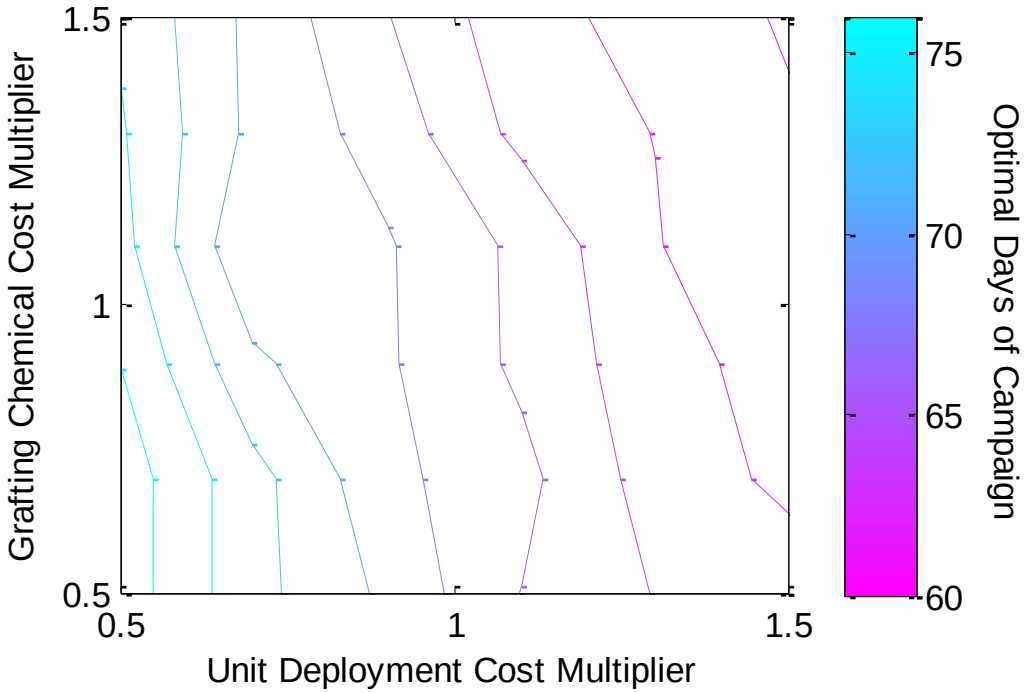

Figure 4.4: Optimal Days of Campaign as a Function of Deployment and Grafting Chemical Cost Multipliers

The cost of adsorbent deployment is a complicated function of the length of the immersion. Shorter campaigns require a smaller adsorbent field with a higher servicing rate, meaning that less uranium is recovered per deployment event but more uranium is recovered per unit area of the field as the campaign is shortened. Since the unit deployment cost includes the capital, operating, and decommissioning cost of deployment activities, shorter immersion times become favorable as the unit deployment cost increases. Length of campaign has little effect on the operations component of the deployment cost, which is dominated by the sailors' labor expense. The increased frequency of service does increase this cost due to a greater number of ships required. This is however overshadowed by the significant decrease in capital cost associated with a smaller field requiring fewer expensive chains.

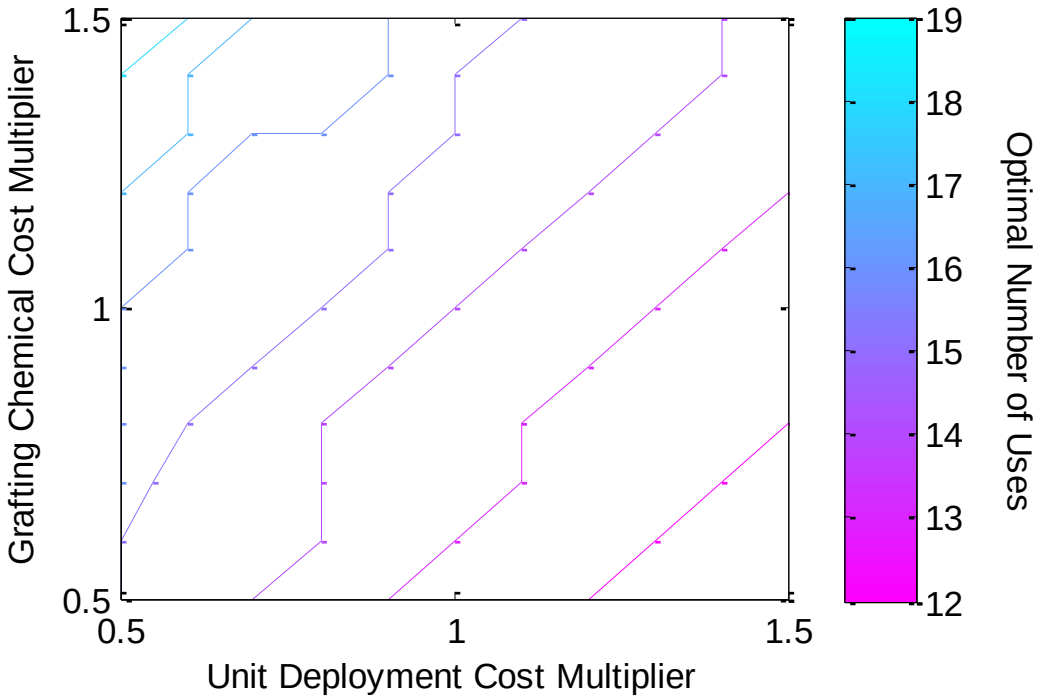

Figure 4.5: Optimal Number of Uses as a Function of Deployment and Grafting Chemical Cost Multipliers

As expected, higher deployment costs favor fewer uses of the same mass of adsorbent. Degradation of the adsorbent causes lower uranium uptake with each use and at high deployment costs this decreased mass of uranium is no longer worth obtaining.

Conversely, increasing the grafting chemical cost increases the optimal number of uses. As the adsorbent becomes more expensive to produce it is increasingly advantageous to reuse it a higher number of times.

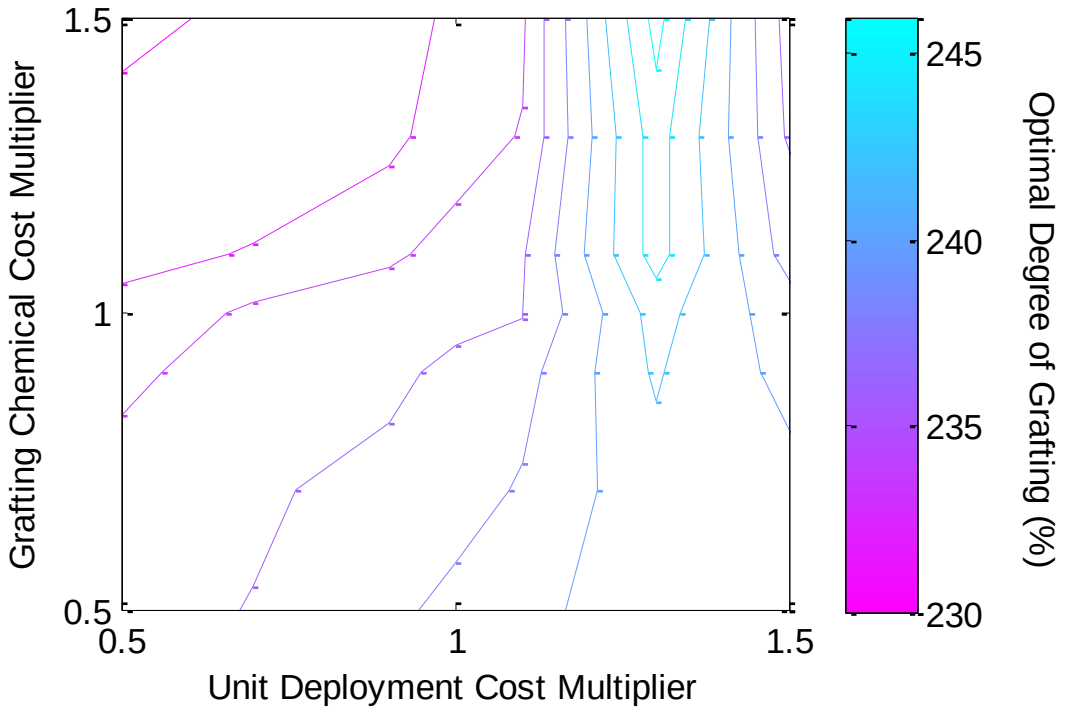

Figure 4.6: Optimal Degree of Grafting as a Function of Deployment and Grafting Chemical Cost Multipliers

Several competing factors lead to the complex topology seen in figure 4.6 Increasing the grafting chemical costs favors lower degrees of grafting if everything else is held fixed. As the price of the grafting chemicals rises, the marginal uranium obtained by higher degrees of grafting does not outweigh the added production expense.

Increasing the unit deployment cost appears to have the opposite effect. When the cost associated with each deployment of a unit mass of adsorbent increases, it is advantageous to recover as much uranium as possible. It was observed that the optimal length of campaign decreased with increasing deployment cost, due to field size expenses, as did the number of uses. Increasing the grafting percentage improves the uranium recovery, so a tendency toward higher DOG at higher deployment costs is also seen in Figure 4.6.

It can be observed that around the point (1,1), which corresponds to the reference conditions, the optimal degree of grafting is around the 235% predicted earlier. To the left and above this point the optimal DOG decreases consistently. To the right and below this point the optimal DOG increases until the increased uranium recovery associated with high DOG is outweighed by the chemical cost savings associated with low DOGs.

FIXED NUMBER OF USES

The next sensitivity analysis constrains one part of the parameter space to investigate how other decision variables are affected. This sensitivity considers the hypothesis that loss in uptake due to biofouling is a function of both temperature and time in the ocean. The number of uses is removed from the optimization and is analyzed at three constant values, one, six, and fifteen. A single use scenario is considered in the case that degradation turns out to be significantly higher than expected. Six uses of a unit mass of adsorbent are considered as a historical relevant base case. Fifteen uses are also considered as this is the optimal number of uses under the time and temperature dependent biofouling conditions. The minimum uranium production cost and its corresponding optimal length of campaign and ocean temperature for these three use scenarios are displayed in Figures 4.7 and 4.8.

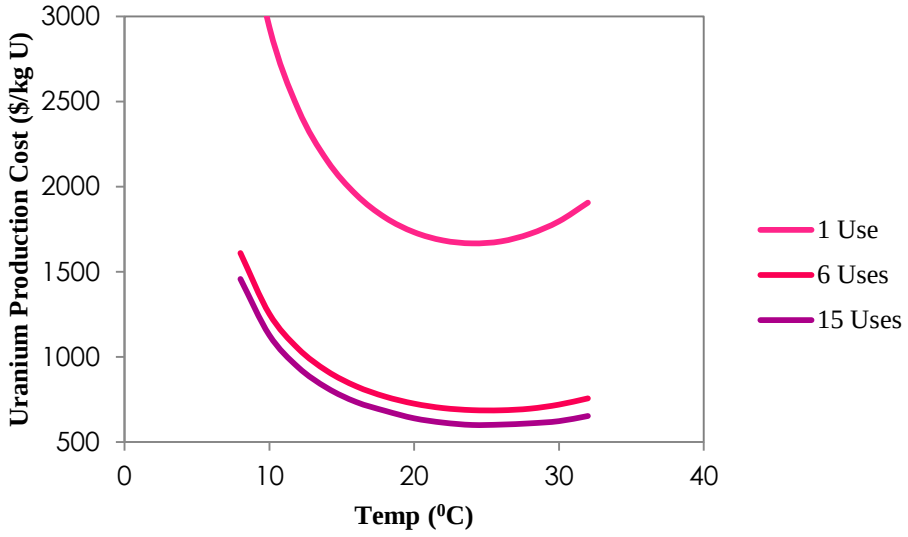

Figure 4.7: Minimized Uranium Production Cost as a Function of Temperature for a Fixed Number of Uses

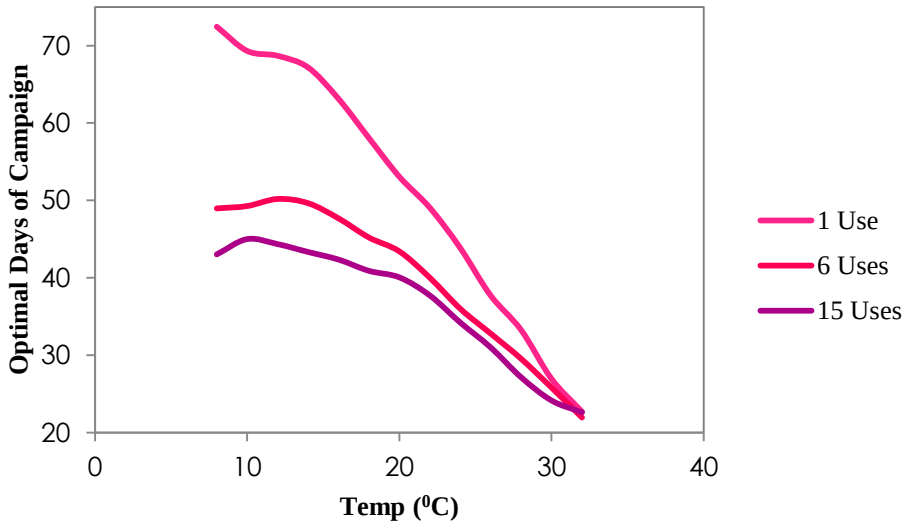

Figure 4.8: Optimal Days of Campaign as a Function of Temperature for a Fixed Number of Uses

As expected, the cost of uranium recovery decreases as the number of uses increases and approaches the optimal value in the reference case conditions. The increase

in total uranium uptake over the adsorbent lifetime recoups more of the costly production expense. Consequently, fewer uses of the adsorbent favor longer campaign lengths in order to recover as much uranium as possible. This effect is most dramatic in the case of a single adsorbent use. Subsequent re-uses of the adsorbent favor shorter campaign lengths because all of the micro-organisms are assumed to be removed by the harsh acids used in the elution process; on the next deployment the effects of biofouling therefore again start at zero. In the case of many uses, the loss due to biofouling exceeds the loss in uptake suffered from acidic degradation if the campaign is lengthy. When re-use is not an option however, it is most advantageous to allow the adsorbent to approach its capacity, even though this capacity has been lowered due to biofouling. This trend does not continue as the ocean temperature approaches the maximum considered, where the biofouling becomes so severe that even in a single use scenario favors short campaign lengths.

CONCLUSION

This thesis presented the successful optimization of deployment conditions to minimize the uranium production cost for a passive recovery system. First the system under consideration, as developed by Oak Ridge and Pacific Northwest National Labs, was described. Next a literature review was conducted in order to determine an appropriate optimization algorithm for the problem at hand. Given the complexity and platform of the cost calculation it was determined that the problem be treated as a black box optimization. Therefore derivative free optimization algorithms were studied.

The parameter space of the problem was described in detail. The base case includes the optimization of three decision variables each with a unique influence on adsorbent performance: days of campaign the adsorbent spends in the ocean, number of uses of each adsorbent unit mass before disposal, and degree of functional ligand grafting. Additional cases consider the temperature of ocean water and the effects this has on both adsorbent uranium capacity and the loss due to biofouling. Warmer waters are known to increase the capacity of the adsorbent to take up uranium but also presumably enhance the effects of biofouling; these competing effects were explored in the optimization. An alternative elution process using potentially milder chemicals is also described.

Due to the complex nature of the calculation the economic estimate was treated as a black box, thus a literature review was conducted to search for applicable algorithms. Eventually, the Nelder-Mead simplex method, a true derivative free algorithm, was adopted. Since each iteration only requires one new objective function value, the run time was low enough such that a high convergence criteria could be set.

Optimization of the base case was conducted to yield a minimum uranium production cost 11% lower than the historical reference case cost. A brute force calculation with increasingly smaller ranges and interval constraints was conducted to verify this result.

The first addition to the reference case was the presence of biofouling, the growth of micro-organisms on the adsorbent interfering with its ability to uptake uranium. Since very preliminary data exists, the known data set was first used without any extrapolation to consider the loss in uptake due to biofouling, independent of both length of campaign and temperature of the ocean. The optimization of a system including this constant loss in uptake resulted in a higher minimized uranium production cost with very similar optimal deployment conditions.

Next the loss due to biofouling was hypothesized to be tied to the temperature dependent growth of marine bacteria. The temperature at which the increase in uranium uptake was outweighed by increased biofouling was found to be around 22^0C. But due to the provisional nature of both the limited data and the temperature dependent hypothesis, further experimentation is needed in this area to reduce uncertainty.

The effects of biofouling were lastly considered to be a function of both time spent in the ocean and temperature of the water. In this case the optimal temperature was found to be slightly higher, 25^0C, as the increase in growth due to temperatures was offset by a shorter campaign. The most notable conclusion resulting from this analysis was the realization that if biofouling does turn out to be dependent on length of campaign, particularly in a near liner fashion, then the improvement of uptake kinetics will become an important objective for reducing uranium production costs.

Lastly, the bicarbonate elution process was explored and optimized. Due to significant uncertainty the adsorbent durability under in this newly developed process,

multiple degradation rates were explored. If the degradation rate is identical to the reference acidic process the uranium production costs will decrease by approximately 20%. The break even analysis with respect to the degradation rate associated with each elution process illustrated the fact that bicarbonate degradation rates need to become quite high before the acidic process is more favorable.

Finally, to reflect the reality that the technology surrounding this uranium recovery process is constantly evolving and subject to significant uncertainty, sensitivity analyses were conducted to provide intuition for determining optimal deployment conditions.

First the cost associated with deploying a unit mass of adsorbent and the grafting chemical costs for the base case are multiplied by a factor ranging from 0.5 to 1.5. These changes in input costs have significant impacts on the optimal decision variable values indicating that the optimal scenario will continue to change with the technology. Increasing both of these costs generally favors a shorter length of campaign. Since deployment capital cost is more sensitive to changes in field size than the operating cost, the more frequent servicing of smaller fields necessary for shorter immersion times becomes advantageous. Increasing the deployment cost also decreases the optimal number of adsorbent uses because the degradation suffered with each use becomes increasingly important as each recovery event is more expensive. Increasing grafting costs though favors a greater number of uses because the costly production expense must now be offset by increased uranium recovery through numerous uses. The optimal degree of grafting also has competing costs with respect to these two cost increases.

Although many cost estimates exist for uranium recovery from seawater, a systematic optimization framework has never been developed. The novelty of this research is the application of this existing optimization algorithm in order to illuminate

areas of R&D focus moving forward. This cost minimization through system and design parameter alterations indicates what type of return would be achieved by improving various components of the system. For example it has been demonstrated that significant cost savings would result from improved kinetics if the effects of biofouling do turn out to be time dependent.

The results concluded in this thesis are important factors to consider when directing future research. Furthermore, even as the technology continues to evolve, the methodology developed for this optimization will remain relevant. While minor changes may need to be made to reflect updates, the application of this optimization algorithm is robust with regard to changes in adsorbent performance.

APPENDIX

Table A1: Calculated cost component values for the base case

Process Step	Cost Component	Value Calculated	Units
Adsorbent Production	Capital Cost	$935	tonne adsorbent produced
	O&M Cost	$5,181	tonne adsorbent produced
	D&D Cost	$31	tonne adsorbent produced
Mooring and Deployment	Capital Cost	$249	tonne adsorbent deployed
	O&M Cost	$338	tonne adsorbent deployed
	D&D Cost	$8	tonne adsorbent deployed
Elution and Regeneration	Capital Cost	$34	tonne adsorbent deployed
	O&M Cost	$62	tonne adsorbent deployed
	D&D Cost	$1	tonne adsorbent deployed

Table A2: Scaling Factors used in Economies of Scale Calculation from Previous Cost Estimate [15]

Equipment/Facility Type	Exponent Value
Solvent Extraction Facility	0.73
Melt Spinning Equipment	0.46
E-Beam	0.26
Chemical Plants (All Others)	0.67

Some costs are determined relative to cost of necessary equipment or the fixed capital investment (FCI). The FCI consists of the delivered equipment in addition to all of the miscellaneous costs calculated from it.

Table A3: Factors used to estimate Overnight Capital Cost [15]

Service or Expense	Cost	Unit
Delivery of Equipment	10	% of Purchased Equipment
Equip. Installation	39	% of Delivered Equip
Instrumentation and Controls	26	% of Delivered Equip
Piping	31	% of Delivered Equip
Electrical Systems	10	% of Delivered Equip
Buildings	29	% of Delivered Equip
Yard Improvements	12	% of Delivered Equip
Service Facilities	55	% of Delivered Equip
Engineering & Supervision	32	% of Delivered Equip
Construction Expenses	34	% of Delivered Equip
Legal Expenses	4	% of Delivered Equip
Contractor's Fee	19	% of Delivered Equip
Auxiliary Facilities	50	% of Delivered Equip
Contingency Cost	0.1	Times Total Cost
Land	0.015	Fraction of FCI

Table A4: Chemical Consumption Values for Adsorbent Production

Chemical	Tonne Required per Tonne Adsorbent	Recyclability
High Density Polyethylene	0.29	0%
Polylactic Acid	0.12	90%
Tetrahydrofuran	0.29	90%
100% Hydroxylamine Hydrochloride	0.70	0%
100% Acrylonitrile	0.54	0%
1:1 Water-Methanol	3.51	90%
Dimethylsulfoxide	0.24	90%
99.5% Itaconic Acid	0.18	0%

Table A5: Chemical and Material Costs from Vendor Quotes and Previous cost Estimate [15] and [17]

Chemical	Average Cost	Unit	Std. Dev
Acrylonitrile	$588	metric ton	$259
Ammonia	$341	metric ton	$148
Ammonium Hydroxide	$1,973	metric ton	$689
Calcium Oxide (Lime)	$107	metric ton	$15
Dimethyl Sulfoxide	$1,659	metric ton	$624
Filter Aid (Diatomite)	$325	metric ton	$59
Hydrochloric Acid	$148	metric ton	$58
Hydroxylamine HCl	$1,558	metric ton	$208
Itaconic Acid	$1,850	metric ton	$301
Kerosene	$2	$/gallon	$1
Magnesium Oxide	$598	metric ton	$121
Methacrylic Acid	$3,444	metric ton	$518
Methanol	$284	metric ton	$127
Nitric Acid	$284	metric ton	$47
Polyethylene (HDPE)	$1,467	metric ton	$280
Polylactic Acid (PLA)	$1,978	metric ton	$285
Potassium Bicarbonate	$982	metric ton	$141
Potassium Hydroxide	$1,045	metric ton	$21
Sodium Carbonate	$149	metric ton	$43
Sodium Chloride (non-food grade)	$100	metric ton	$15
Sodium Hydroxide	$483	metric ton	$113
Sulfuric Acid	$63	metric ton	$20
Tetrahydrofuran (THF)	$3,589	metric ton	$538
Tributyl Phosphate	$6,419	metric ton	$1,848

Table A6: Utility Prices from Previous Cost Estimates [15]

Chemical	Average Cost	Unit	Std. Dev
Cost of Electricity ($/kWh)	$0.07	kWh	$0.00
Cooling Water ($/1000 m3)	$16	1000 m^3	$2
Process Water	$0.07	metric ton	$0.01
Boiler Water (@ 115 °C)	$3	metric ton	$0.40
Potable Water	$0.28	metric ton	$0.04
Deionized Water	$1	metric ton	$0.16
Low Pressure - 5 barg, 160°C	$32	metric ton	$5
Medium Pressure - 10 barg, 184°C	$32	metric ton	$5
High Pressure - 41 barg, 254°C	$32	metric ton	$5
Primary (filtration)	$44	1000 m3	$7
Secondary (filtration + activated sludge)	$57	1000 m^3	$9
Tertiary (filtration, activated sludge, chemical treatment)	$61	1000 m^3	$9
#2 Heating Oil	$2	gallon	$0.28

Table A7: Factors Used to Estimate Annual O&M Costs from Previous Cost Estimate [15]

Service/Expense	Cost	Unit
Management Staff	0.175	fraction of Operator cost
Maintenance Est.	0.06	fraction of FCI
Operating Supplies Est.	0.011	fraction of FCI
Taxes and Insurance	0.032	fraction of FCI
Contingency	0.1	fraction of total annual cost

Table A8: Values Used to Derive Mooring and Deployment Capital Cost from Chains. [17]

Item	Value	Unit
Total Adsorbent Field	63,044	metric tons
Adsorbent Linear Density	1	kg/meter
Adsorbent Length	60	meters
Width of Braid Adsorbent	0.20	m
Total # of Braids	1,050,741	braid Adsorbents
Chain Length	2120	meters
Chain End Length	100	meters
Braid Spacing	8	meters
Braids/Chain	240	
Number of Rows	218	Rows
Row Spacing	70	
Chains per Row	21	
Chains Required	4578	Chains
Chain Diameter Required	44	mm
Chain Linear Density	43	kg/meter
Chain Unit Price	$33.99	$/m
Chain Buoyance per Braid	333.95	
Density of HDPE	953.00	kg/m3
Net Buoyant Force of Single Braid	44.47	N
Total Chain Buoyance per Chain	10,672.62	N/chain
Drag Force	54,098.23	N
Mass of Anchor per Chain	22,384.44	kg
Anchor (Old Chain)	520.57	m
Chain Unit Price	$96.74	$/m
Total Chain Cost for Field	560,432,314	$

Table A9: Values Used to Derive Mooring and Deployment Capital Cost from Ships [17]

Item	Value	Unit
Small Ships		
Required Daily Chain Recovery Rate	73	chains/day
Hours of Boat Operation per Day	9	hours/day
Chain Recovery Speed	4	m/min
Time to Recover Each Chain	9	hours
Chains Recovered by each Boat per day	1	Chains/boat/day
Tons Ads on each Chain	14	tons ads/chain
Tons U Recovered from each Chain	0.05	tons U/chain
Number of Boats Required	73	Small Boats
Boat Capacity (Dead weight)	965	tonnes
Specific Fuel Oil Consumption	163	g/bhp-hr
Cost of Each Small Boat	539,824	2010$/boat
Total Small Boat Cost	39,407,152	2010$
Mother Ship		
Chemicals Carried	2,573	tonnes
Tanks Carried	800	tonnes
Total Loaded Ads Weight	70,407	tonnes
Amount of Spent Ads (1/recycles * amount of adsorbent the mothership comes in contact with in 30days)	5,254	tonnes
Product Collected in 30 Days on Mothership	3,681	tonnes
Weight Per Chain's ads after immersion	16	tonnes

Adsorbent (7 days' worth)	17,149	tonnes
Total Weight	20,522	tonnes
Total Cost	43,532,008	$
Supply Ship		
Chemicals Carried	2,573	tonnes
Tanks Carried	800	tonnes
adsorbent product (30 days' worth + 1 / number of uses * amount of ads mothership is holding)	8,935	tonnes
Total Weight	12,308	tonnes
Total Cost	29,531,192	$
Cost of All Ships	112,470,352	$

Table A10: Values Used to Calculate Mooring and Deployment O&M Cost [17]

Item	Input per Ton Deployed	Unit
NY Harbor #2 Heating Oil for Small Boats	8	gallons
NY Harbor #2 Heating Oil for Mothership	30	gallons
NY Harbor #2 Heating Oil for Supply Ships	19	gallons
Captains' Labor	1	captain/ship
Sailor/Workers' Labor	16	workers/ship
Off Shore Lease	1.77E-03	km^2
Other Operating Consumables	0.04	Times Capital
Contingency	0.1	Times O&M

GLOSSARY

Financial Parameters Symbols

Symbol	Meaning	Units
AF	Amortization Factor	n/a
t	**time**	
T_{proj}	Total Years of Project	years
t_i	Length of Immersion	days
T_e	Length of Elution	days
T_s	Length of Down Time on Ship	days
T_c	Length of Total Cycles	days
T_P	Point in Time at which Adsorbent is Produced	days
$t_{M,n}$	Point in Time at which Adsorbent is Moored for the nth Time	days
$t_{E,n}$	Point in Time at which Adsorbent is Eluted for the nth Time	days
$t_{U,n}$	Point in Time at which Uranium is Obtained for the nth Time	days
i	**Interest Rate**	
i_d	Discount Rate	%
i_{SF}	Interest Rate of Sinking Fund	%
i_c	Interest Rate of Capital	%
CC	**Capital Cost**	
OCC_{prod}	Overnight Capital Cost of Adsorbent Production	$/production facility of necessary size
CC_{prod}	Capital Cost of Adsorbent Production Amortized over Project Lifetime	$/year
cc_{prod}	Capital Cost of Adsorbent Production per Unit of Adsorbent Produced	$/ton ads produced
OCC_{moor}	Overnight Capital Cost of Mooring	$/mooring facility of necessary size
CC_{moor}	Capital Cost of Mooring Amortized over Project Lifetime	$/year

cc_{moor}	Capital Cost of Mooring per Unit of Adsorbent Deployed	$/ton ads deployed
OCC_{elut}	Overnight Capital Cost of Elution	$/elution facility of necessary size
CC_{elut}	Capital Cost of Elution Amortized over Project Lifetime	$/year
cc_{elut}	Capital Cost of Elution per Unit of Adsorbent Deployed	$/ton ads deployed
OC	**Operating Cost**	
OC_{prod}	Annual Operating Cost of Adsorbent Production	$/year
oc_{prod}	Operating Cost of Production per Unit of Adsorbent Produced	$/ton ads produced
OC_{moor}	Annual Operating Cost of Mooring	$/year
oc_{moor}	Operating Cost of Mooring per Unit of Adsorbent Deployed	$/ton ads deployed
OC_{elut}	Annual Operating Cost of Elution	$/year
oc_{elut}	Operating Cost of Elution per Unit of Adsorbent Deployed	$/ton ads deployed
DC	**Decontamination and Decommissioning Cost**	
ODC_{prod}	Overnight Decontamination and Decommissioning Cost of Adsorbent Production	$/decommission of production facility of necessary size
DC_{prod}	Decontamination and Decommissioning Cost of Adsorbent Production Amortized over Project Lifetime	$/year
dc_{prod}	Decontamination and Decommissioning Cost per Unit of Adsorbent Produced	$/ton ads produced
ODC_{moor}	Overnight Decontamination and Decommissioning Cost of Mooring	$/decommission mooring facility of necessary size
DC_{moor}	Decontamination and Decommissioning Cost of Mooring Amortized over Project Lifetime	$/year
dc_{moor}	Decontamination and Decommissioning Cost per Unit of Adsorbent Deployed	$/ton ads deployed
ODC_{elut}	Overnight Decontamination and Decommissioning Cost of Elution	$/decommission elution facility of necessary size
DC_{elut}	Decontamination and Decommissioning Cost of Elution Amortized over Project Lifetime	$/year
dc_{elut}	Decontamination and Decommissioning Cost per Unit of Adsorbent Deployed	$/ton ads deployed
UC	**Unit Cost**	
uc_{prod}	Unit Cost of Adsorbent Production per Unit of Adsorbent Produced	$/ton ads produced

uc_{moor}	Unit Cost of Mooring per Unit of Adsorbent Deployed	$/ton ads deployed
uc_{elut}	Unit Cost of Elution per Unit of Adsorbent Deployed	$/ton ads deployed
luc_{prod}	Lifecycle Unit Cost of Adsorbent Production per Unit of Adsorbent Produced	$/ton ads produced
luc_{moor}	Lifecycle Unit Cost of Mooring per Unit of Adsorbent Produced	$/ton ads produced
luc_{elut}	Lifecycle Unit Cost of Elution per Unit of Adsorbent Produced	$/ton ads produced

Production Symbols

Symbol	Meaning	Units
	System Parameters	
N	Number of Uses of Adsorbent	n/a
d	Degradation Rate of Adsorbent per Re-use	%
g	Degree of Grafting of Ligand (DOG)	%
U_{req}	Annual Uranium Output Production Required	tonnes U/year
t_{prod}	Years of Production	years
K_D	Half Saturation Time of Adsorbent Uptake	days
β_{max}	Saturation Point of Adsorbent	kg U/ton ads/days^2
M	**Mass of Adsorbent**	
M_{inv}	Total Inventory of Adsorbent (including out of water)	tonnes adsorbent
M_{field}	Total Amount of Adsorbent in the Ocean (Steady State)	tonnes adsorbent
m_{dep}	Total Mass Deployed per Year	tons ads/year
m_{prod}	Annual Amount of Adsorbent Produced	tons ads/year
C	**Capacity**	
C_n	Uptake of Adsorbent on the nth Use	kg U/ton ads
$C_{ads\ life}$	Total Uptake of Adsorbent from All Deployments	kg U/ton ads
$C_{b,n}$	Uptake of Adsorbent on the nth Use Accounting for Biofouling	kg U/ton ads
C_{max}	U Capacity of Fresh Ads	kg U/ton ads

References

[1] T-L. Ku and K.G. Knauss and G.G. Mathieu, "Uranium in Open Ocean: Concentration and Isotopic Composition," *Deep Sea Research,* **vol.24,** *11,* 1005-1017 (1977).

[2] Schneider, E. and Sachde, D. Uranium from Seawater by a Braided Polymer Adsorbent System," *Science and Global Security: The Technical Basis for Arms Control, Disarmament, and Nonproliferation Initiatives,* **vol. 21,** *2,* 134-163 (2013).

[3] Kirkpatrick, S.; Gelatt, C.D.; Vecchi,M.P. 1983. Optimization by Simulated Annealing. *Science*. **vol**. **220**, No. 4598. pp.671-680.

[4] Ingber, L. Simulated Annealing: Practice Versus Theory. *Mathl. Comput. Modeling*. **vol**. 18, No. 11, pp. 29-57. (1993)

[5] Whitley, D. A Genetic Algorithm Tutorial. *Statistics and Computing*. **vol**. **4,** 65-85. (1994)

[6] Blum, C. Ant Colony Optimization: Introduction and Recent Trends. *Physics of Life Reviews*. 2. Pp 353-373.(2005.)

[7] Wong, E., Summers, P., Ku, R., Xie, P. Ant Colony Optimization. Class lecture. University of California at Los Angeles.(2011).

[8] Dennis, J.E. and Schnabel, R. Numerical Methods for Unconstrained Optimization and Nonlinear Equations. *Society for Industrial and Applied Mathematics*. Pretnice-Hall, Englewood Cliffs, NJ.(1996).

[9] J.A. Nelder and R. Mead. "A Simplex Method fo Function Minimization," *The Computer Journal,* **vol. 7,** 4, 308-313 (1965).

[10] Leps, M. and Sejnoha, M. New Approach to Optimization of Reinforce Concrete Beams. *Computers and Structures*. **vol**. **81**. Issues 18-19. Pp 1957-1966.(2003).

[11] Jayabalan, V. and Chaudhuri, D. Cost Optimization of Maintenance Scheduling for a System with Assured Reliability. *IEEE Transactions on Reliability*. **vol**. **41**, No.1. Pp 21-25.(1992).

[12] Santarelli, M. and Pellegrino, D. Mathematical Optimization of a RES-H_2 Plant Using a Black Box Algorithm. *Renewable Energy*. **vol**. **30**. Pp 493-510.(2004).

[13] Abendroth, R. and Salmon, C. Sensitivity Study of Optimum RC Restrained End T-Sections. *Journal of Structural Engineering*. **vol**. **112**. Pp. 1928-1943.(1986).

[14] Park, C. *Contemporary Engineering Economics.* Upper Saddle River, New Jersey. Pearson Education Inc. 220-227.

[15] Schneider, E. and Sachde, D. Cost and Uncertainty Analysis of an Adsorbent Braid System for Uranium Recovery from Seawater. Unpublished Master's Thesis. The University of Texas at Austin. (2011).

[16] Economic Modeling Working Group of the Generation IV International Forum. Cost Estimate Guidelines for Generation IV Nuclear Energy Systems. Revision 4.2. (2007).

[17] Lindner, H. A Cost Estimate for Uranium Recovery from Seawater Using a Chitin Nanomat Adsorbent. Unpublished Master's Thesis. The University of Texas at Austin. (2014).

[18] Saito, T., Brown, S., Chatterjee, S., Kim, J., Tsouris, C., Mayes, R., Kuo,L-J, Gill, G., Oyola, Y., Janke, C. and Dai, S., "Uranium recovery from seawater: development of fiber adsorbents prepared via atom-transfer radical polymerization," Journal of Materials Chemistry A, vol 2, 14674-14681 (2014).

[19] G. A. Gill and L-J. Kuo and J. Wood and C. Janke, "Complete Laboratory Evaluation and Issue a Report on the Impact of Temperature on Uranium Adsorption," Milestone Letter Report. Sep.20, 2014.

[20] DOE Office of Nuclear Energy, "Fuel resources Uranium From Seawater Program," *Program Review Document,* Oak Ridge National Laboratory, Jun. 13 2013.

[21] C. Janke and S. Das and R. Mayes "Preparation of most promising braided and/or textile-based adsorbents for seawater testing," Milestone Letter Report. Feb.28, 2014

[22] G. Bonheyo and J. Park, **"**How Biofouling Impacts Uranium Sorbent Material Performances and What Can Be Done to Mitigate the effects." *American Chemical Society National Meeting.* Dencer, CO. Mar. 23, 2015.

[23] P.A. White and J. Kalff and J. R. Rassmussen and J.M. Gasol, "The Effect of Temperature and Algal Biomass on Bacterial Production and Specific Growth Rate in Freshwater and Marine Habitats," *Microbrial Ecology*, **vol. 21,** *1,*99-118 (1991).

[24] H-B. Pan and W. Liao and C. Wai and Y. Oyola and C. J. Janke and G. Tian and L. Rao, "Carbonate-H2O2 leaching for Sequestering Uranium form Seawater," *Dalton Transactions,* **vol. 43,***28,* 10713-10718 (2014).

[25] Armijo, L. Minimization of Functions Having Lipschitz Continuouse First Partial Derivatives. *Pacific Journal of Math*. **vol.16**,*1*, 1-3. (1966).

[26] Broyden, C., Dennis, J. and More, J. On the Local and Superliner Convergence of Quasi-Newton Methods. *Journal of Applied Mathematics.* **vol.12,**3,223-245.

[27] J.C. Lagarias and J. A. Reeds and M. H. Wright and P. E. Wright, "Convergence Properties of the Nelder-mead Simplex Method in Low Dimensions," *Society for Industrial and Applied Mathematics Journal on Optimization,* **vol. 9,** *1,* 112-147. (1998).

[28] Hansen, N. "Benchmarking the Nelder-Mead Downhill Simplex Algorithm with Many Local Restarts." *Proceedings of the 11th Annual*

Conference Companion on Genetic and Evolutionary Computation. Montreal, Canada. (2009).

[29] Tamada. M., Seko, N., Kasa, N., and Shimizu, T. Cost Estimation of Uranium Recovery from Seawater with System of Braid Type Adsorbent. *Transactions of the Atomic Energy Society of Japan.* 358-363. (2006)

Vita

Maggie Byers, born Margaret Elise Flicker, grew up in Orange County, CA. She received her B.S. in chemistry from the University of California at Los Angeles in 2013. In pursuing her desires to apply her scientific background to environmental concerns, she joined Dr. Erich Schneider's nuclear fuel cycle group in the fall of 2013. After finishing this master's thesis she plans to continue on to obtain her PhD in fuel cycle work in the same program.

Permanent address (or email): MEFlicker@UTexas.edu

This thesis was typed by Margaret Byers